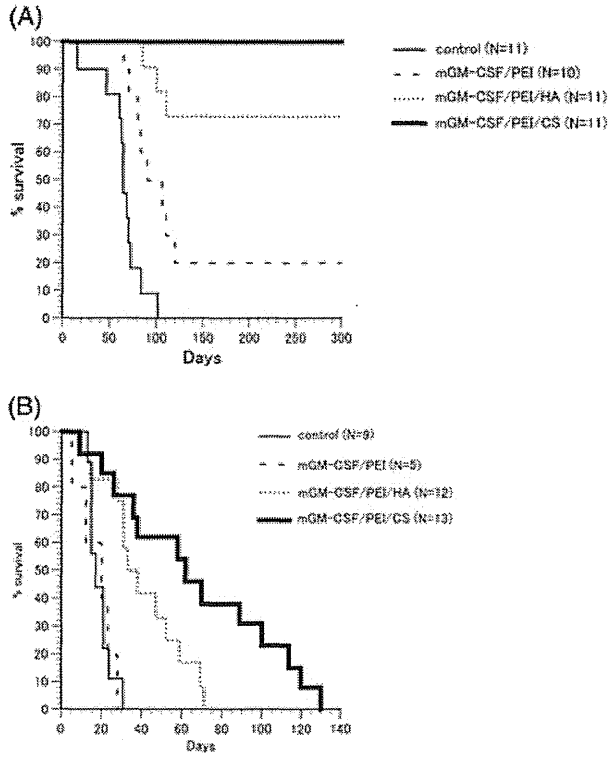

Figure 5. (A) Kaplan–Meier survival curve of antitumor effects of mGM-CSF/PEI/HA or 10-kDa CS ternary complex in mice bearing subcutaneous OVHM tumors. The complex (100 μg/500 μl) was intratumorally administered into 5–8 mm diameter subcutaneous tumors over 3 consecutive days after subcutaneous inoculation of OVHM cells (1×10^6 cells). (B) Kaplan–Meier survival curve of antitumor effect of mGM-CSF/PEI/HA or 10-kDa CS ternary complex in mice bearing intraperitoneal OVHM tumors. The complex (100 μg/7 ml) was intraperitoneally and subcutaneously administered six times daily after the intraperitoneal inoculation of OVHM cells (1×10^6 cells).

present study because that with chitosan is lower in transfection efficiency [19,20]. Ternary complexes coated with seamless, bovine or shark ≥ 14-kDa CSs were reported previously [21–23]. We have reported here for the first time use of a 10-kDa fraction of CS as an anionic component of ternary complex, and have shown that ternary complex coated with this fraction exhibited higher luciferase activity than when fractions of CS ≥ 14-kDa or high-molecular-weight HA were used. Furthermore, the 10-kDa fraction CS-coated mGM-CSF complex inhibited the growth of intraperitoneal and subcutaneous tumor in a syngeneic mouse model to a greater extent than did ternary mGM-CSF/PEI/HA complex. In the present study, the CS polymer was higher in gene expression efficiency than the HA polymer, and the size of the CS polymer was approximately two-thirds of that of the HA polymer. Regarding the size after the polymer processing being small, it is suggested to be advantageous for uptake in the cell after attachment to the CD44 receptor on the cell membrane. Furthermore, as we reported previously [24,25], addition of polyanions, such as HA and polyethylene glycol derivatives, to the DNA/polycation complex caused the loosening of the complex particles and improved transcription efficiency by the effect of the charge balance in the polyampholyte. The addition of CS would thus also loosen the complex. The loosening effect of CS would be stronger than that with HA because CS has many strong acid (sulfuric acid) pendants along the chain.

Three intratumoral injections of 100 μg of ternary mGM-CSF/PEI/CS complex induced complete tumor reduction in all subcutaneous tumors. There are many types of tumors that can be directly injected in intratumoral fashion, such as head and neck cancers, thyroid cancer, esophageal cancer, breast cancer and skin cancer, as well as gynecological cancers, such as vaginal cancer, vulvar cancer and cervical cancer. Deep organ cancers such as lung cancer, liver cancer, brain tumor and others and digestive organ cancers such as gastric cancers, colon cancers, and others are, respectively, computed tomography- or echo-guided and endoscopically-injectable tumors. These tumors can therefore be radically treated only with three intratumoral injections of ternary GM-CSF/PEI/CS complex. This local treatment procedure appears promising because radical surgery for these tumors often features severe postoperative complications, such as behavioural disorders, dysphagia, eating disorders, weight loss, incontinence and cosmetic problems, which often decrease quality of life and make full social rehabilitation impossible. Our method of ternary complex gene therapy by intratumoral injection does not require hospitalization

DOI: 10.1002/jgm

and could radically cure any cancer subject to monitoring visually or by echographic, endoscopic, computed tomography or other types of monitoring in the outpatient clinic. This gene therapy could reduce the physical and financial burden on patients, as well as national medical expenses. Local intratumoral injection by GM-CSF/PEI/CS ternary complex thus has the potential to replace surgery for locally injectable tumors in the near future. Furthermore, it appears very likely that it will become an important method of treatment in place of anticancer drugs with the further development of systemic treatment of cancers.

Acknowledgements

This research was supported by a Grant-in-Aid from the Ministry of Education, Science, Sports, and Culture, Japan, R&D for Promoting Innovation in Regions, and the Integrated Center for Science of Ehime University. We thank K. Oka for preparing the culture medium. We thank Mr Kubo, Professor Yoshikawa, Professor Kawakami and Professor Hashida (Kyoto University) for their great help in ζ-potential measurements. We also thank Seikagaku Corporation for supplying CSs and hyaluronic acid. The authors declare that there are no conflicts of interest.

References

1. Hamada K, Desaki J, Nakagawa K, *et al.* Carrier cell-mediated infection of a replication-competent adenovirus for cancer gene therapy. *Mol Ther* 2007; **15**: 1121–1128.
2. Plank C, Mechtler K, Szoka FC Jr, Wagner E. Activation of the complement system by synthetic DNA complexes: a potential barrier for intravenous gene delivery. *Hum Gene Ther* 1996; **12**: 1437–1446.
3. Maruyama K, Iwasaki F, Takizawa T, *et al.* Novel receptor-mediated gene delivery system comprising plasmid/protamine/sugar-containing polyanion ternary complex. *Biomaterials* 2004; **16**: 3267–3273.
4. Koyama Y, Yamada E, Ito T, Mizutani Y, Yamaoka T. Plasmid/polycation complexes for receptor-mediated gene delivery. *Macromol Biosci* 2002; **2**: 251–256.
5. Finsinger D, Remy JS, Erbacher P, Koch C, Plank C. Protective copolymers for nonviral gene vectors: synthesis, vector characterization and application in gene delivery. *Gene Ther* 2000; **7**: 1183–1192.
6. Ito T, Iida-Tanaka N, Niidome T, *et al.* Hyaluronic acid and its derivative as a multi-functional gene expression enhancer: protection from non-specific interactions, adhesion to targeted cells, and transcriptional activation. *J Control Release* 2006; **112**: 382–388.
7. Koyama Y, Yamashita M, Iida-Tanaka N, Ito T. Enhancement of transcriptional activity of DNA complexes by amphoteric PEG derivative. *Biomacromolecules* 2006; **7**: 1274–1279.
8. Sakae M, Ito T, Yoshihara C, *et al.* Highly efficient in vivo gene transfection by plasmid/PEI complexes coated by anionic PEG derivatives bearing carboxyl groups and RGD peptide. *Biomed Pharmacother* 2008; **62**: 448–453.
9. Ito T, Iida-Tanaka N, Koyama Y. Efficient in vivo gene transfection by stable DNA/PEI complexes coated by hyaluronic acid. *J Drug Target* 2008; **16**: 276–281.
10. Trubetskoy VS, Loomis A, Slattum PM, Hagstrom JE, Budker VG, Wolff JA. Caged DNA does not aggregate in high ionic strength solutions. *Bioconjug Chem* 1999; **10**: 624–628.
11. Ito T, Yoshihara C, Hamada K, Koyama Y. DNA/polyethyleneimine/hyaluronic acid small complex particles and tumor suppression in mice. *Biomaterials* 2010; **31**: 2912–2918.
12. Sugahara KN, Hirata T, Tanaka T, *et al.* Chondroitin sulfate E fragments enhance CD44 cleavage and CD44-dependent motility in tumor cells. *Cancer Res* 2008; **68**: 7191–7199.
13. Henke CA, Roongta U, Mickelson DJ, Knutson JR, McCarthy JB. CD44-related chondroitin sulfate proteoglycan, a cell surface receptor implicated with tumor cell invasion, mediates endothelial cell migration on fibrinogen and invasion into a fibrin matrix. *J Clin Invest* 1996; **97**: 2541–2452.
14. Hirabayashi Y, Marugame T. Comparison of time trends in ovary cancer mortality (1990–2006) in the world, from the WHO mortality database. *Jpn J Clin Oncol* 2009; **39**: 860–861.
15. Grzybowski J, Oldak E, Antos-Bielska M, Janiak MK, Pojda Z. New cytokine dressing kinetics of the in vitro rhG-CSF, rhGM-CSF, and rhEGF release from the dressings. *Int J Pharm* 1999; **184**: 173–178.
16. Hamilton JA. Colony-stimulating factors in inflammation and autoimmunity. *Nat Rev Imunol* 2008; **8**: 533–544.
17. Bradbury PA, Shepherd FA. Immunotherapy for lung cancer. *J Thorac Oncol* 2008; **3**: 164–170.
18. Holt GE, Disis ML. Immune modulation as a therapeutic strategy for non-small-cell lung cancer. *Clin Lung Cancer* 2008; **9**: 13–19.
19. Nour El-Din AN, Shkareta L, Talbot BG, Diarra MS, Lacasse P. DNA immunization of dairy cows with the clumping factor A of *Staphylococcus aureus*. *Vaccine* 2006; **24**: 1997–2006.
20. Sezer AD, Akbuga J. Comparison on in vitro characterization of fucospheres and chitosan microspheres encapsulated plasmid DNA (pGM-CSF): formulation design and release characteristics. *AAPS PharmSciTeck* 2009; **10**: 1193–1199.
21. Guilherme MR, Reis AV, Alves BRV, Kunita MH, Rubira AF, Tambourgi EB. Smart hollow microspheres of chondroitin sulfate conjugates and magnetite nanoparticles for magnetic vector. *J Colloid Int Sci* 2010; **352**: 107–113.
22. Lim JJ, Hammoudi TM, Bratt-Leal AM, *et al.* Development of nano- and microscale chondroitin sulfate particles for controlled growth factor delivery. *Acta Biomat* 2011; **7**: 986–995.
23. Bhadra D, Bhadra S, Jain NK. PEGylated peptide dendrimeric carriers for the delivery of antimalarial drug chloroquine phosphate. *Pharm Res* 2006; **23**: 623–633.
24. Yoshihara C, Shew CY, Ito T, Koyama Y. Loosening of DNA/polycation complexes by synthetic polyampholyte to improve the transcription efficiency: effect of charge balance in the polyampholyte. *Biophys J* 2010; **98**: 1257–1266.
25. Ito T, Iida-Tanaka N, Niidome T, *et al.* Hyaluronic acid and its derivative as a multi-functional gene expression enhancer: protection from non-specific interactions, adhesion to targeted cells, and transcriptional activation. *J Control Release* 2006; **112**: 382–388.

Inhibition of PTEN Tumor Suppressor Promotes the Generation of Induced Pluripotent Stem Cells

Jiyuan Liao[1], Tomotoshi Marumoto[1,2], Saori Yamaguchi[1], Shinji Okano[3], Naoki Takeda[4], Chika Sakamoto[1], Hirotaka Kawano[1], Takenobu Nii[1], Shohei Miyamato[1], Yoko Nagai[1], Michiyo Okada[1], Hiroyuki Inoue[1,2], Kohichi Kawahara[5], Akira Suzuki[5], Yoshie Miura[1] and Kenzaburo Tani[1,2]

[1]Division of Molecular and Clinical Genetics, Department of Molecular Genetics, Medical Institute of Bioregulation, Kyushu University, Fukuoka, Japan; [2]Department of Advanced Molecular and Cell Therapy, Kyushu University Hospital, Fukuoka, Japan; [3]Division of Pathophysiological and Experimental Pathology, Department of Pathology, Graduate School of Medical Sciences, Kyushu University, Fukuoka, Japan; [4]Division of Transgenic Technology, Center for Animal Resources and Development, Kumamoto University, Kumamoto, Japan; [5]Division of Cancer Genetics, Department of Molecular Genetics, Medical Institute of Bioregulation, Kyushu University, Fukuoka, Japan

Induced pluripotent stem cells (iPSCs) can be generated from patients with specific diseases by the transduction of reprogramming factors and can be useful as a cell source for cell transplantation therapy for various diseases with impaired organs. However, the low efficiency of iPSC derived from somatic cells (0.01–0.1%) is one of the major problems in the field. The phosphoinositide 3-kinase (PI3K) pathway is thought to be important for self-renewal, proliferation, and maintenance of embryonic stem cells (ESCs), but the contribution of this pathway or its well-known negative regulator, phosphatase, and tensin homolog deleted on chromosome ten (Pten), to somatic cell reprogramming remains largely unknown. Here, we show that activation of the PI3K pathway by the Pten inhibitor, dipotassium bisperoxo(5-hydroxypyridine-2-carboxyl)oxovanadate, improves the efficiency of germline-competent iPSC derivation from mouse somatic cells. This simple method provides a new approach for efficient generation of iPSCs.

Received 28 November 2012; accepted 3 March 2013; advance online publication 9 April 2013. doi:10.1038/mt.2013.60

INTRODUCTION

Mammalian somatic cells can be reprogrammed into induced pluripotent stem cells (iPSCs) by ectopic expression of *Oct3/4* (also known as *Pou5f1*), *Klf4*, and *Sox2* with or without *c-Myc* (hereafter referred to as "OKSM" and "OKS", respectively).[1–4] iPSCs are similar to embryonic stem cells (ESCs) in their morphology, gene expression, and ability to differentiate into the three germ layers *in vitro* and *in vivo*.[1,5] Compared with ESCs, iPSCs avoid ethical controversy and immune rejection and have a great potential to be a cell source for personalized stem cell-based transplantation therapies. However, the efficiency of iPSC generation is quite low (0.01–0.1%), which is one of the obstacles to be overcome.[1–4,6,7] This low efficiency of iPSC generation is considered to be partially due to senescence and apoptosis induced by ectopic expression of OKSM,[8] although the molecular mechanisms involved in somatic cell reprogramming have not been fully elucidated.[1–3,7] Thus, understanding of the molecular mechanisms leading to reprogramming of somatic cells is crucial, and development of a new strategy for efficient iPSC generation is strongly desired.[8]

Numerous studies have shown that the phosphoinositide 3-kinase (PI3K) signaling pathway is required for maintenance of ESC pluripotency by regulating Nanog and Sox2, both of which are transcription factors involved in self-renewal of ESCs.[9–12] In addition, the PI3K pathway is known to be negatively regulated by phosphatase and tensin homolog deleted on chromosome ten (Pten), a well-known tumor suppressor that is deleted or mutated in various types of cancer.[13–16] Recent studies have shown that knockdown of Pten in ESCs promotes self-renewal, as well as cell survival and proliferation,[16–18] indicating that Pten is also involved in the control of stem cell behavior through PI3K regulation.

Here, we report that transient inhibition of Pten by its inhibitor during the process of reprogramming mouse embryonic fibroblasts (MEFs) promotes their proliferation and enhances the efficiency of germline-competent iPSC generation by ectopic expression of OKSM.

RESULTS

To examine whether inhibition of Pten facilitates the reprogramming process for iPSC generation, we first retrovirally transduced OKSM into MEFs lacking Pten ($Pten^{-/-}$ MEFs)[19] and cultured these cells on mitomycin C (MMC)-treated SNL feeders (a SIM mouse embryo-derived thioguanine and ouabain resistant (STO) cell line transformed with neomycin resistance and mouse leukemia inhibitory factor genes) in mouse ESC medium. At about 7 days after OKSM transduction into $Pten^{-/-}$ MEFs, ESC-like round-shaped colonies were observed (**Figure 1a**). We examined the expression of stage-specific mouse embryonic antigen1 (SSEA1), a marker of mouse ESCs, by immunocytochemistry (**Figure 1b,c**).[20] The number of $SSEA1^{+}$ colonies induced by OKSM significantly increased in $Pten^{-/-}$ MEF cultures (103 ± 2) compared with that in $Pten^{+/-}$ and wild-type MEF cultures (40 ± 9 and 21 ± 9, respectively; **Figure 1c**, left panel). Similar results were obtained when OKS were transduced

The first two authors contributed equally to this work.

Correspondence: Kenzaburo Tani, Division of Molecular and Clinical Genetics, Department of Molecular Genetics, Medical Institute of Bioregulation, Kyushu University, 3-1-1 Maidashi, Higashi-ku, Fukuoka, 812–8582, Japan. E-mail: taniken@bioreg.kyushu-u.ac.jp

(15±4 for Pten$^{-/-}$ MEFs, 6±2 for Pten$^{+/-}$ MEFs and 2±1 for wild-type MEFs; **Figure 1c**, right panel).

To confirm that SSEA1$^+$ colonies were derived from a single cell, and not from cell clusters, we replated fewer OKSM-transduced Pten$^{-/-}$ MEFs onto MMC-treated SNL feeders (100 cells per well in a six-well plate) in ESC medium. At 14 days after retroviral transduction, the number of alkaline phosphatase-positive (AP$^+$) colonies was counted. As a result, 71±12 AP$^+$ colonies were generated from Pten$^{-/-}$ MEFs, whereas only 8±1 colonies were generated from wild-type MEFs (**Figure 1d**, left panel), indicating that ~70% of OKSM-transduced Pten$^{-/-}$ MEFs had the potential to become iPSCs. Similar results were obtained when OKS were transduced into Pten$^{-/-}$ MEFs (**Figure 1d**, right panel). These results strongly indicated that the deficiency of Pten significantly increased the number of iPSCs generated by transduction of OKSM or OKS.

Loss of Pten has been shown to activate the PI3K-Akt pathway.[13,21] We next activated the PI3K pathway by expression of phosphatase-deficient Pten mutants that contained a Cys-124 to serine substitution at the phosphatase catalytic center (CS-Pten),[22] or the active myristoylated form of Akt (myr-Akt),[23] and then the efficiency of iPSC generation from wild-type MEFs by OKSM transduction was examined. We observed significantly more AP$^+$ colonies generated from MEFs expressing CS-Pten+OKSM or myr-Akt+OKSM compared with those generated from the control (354±41, 355±10 and 231±25, respectively) (**Figure 2a**). These results indicated that activation of the PI3K pathway in MEFs enhanced the generation of iPSCs by co-expression of OKSM.

It is thought that continuous activation of the PI3K pathway may cause transformation of cells.[24] Therefore, to efficiently and safely generate iPSCs, transient activation of the PI3K pathway combined with transduction of OKSM might be desirable. To establish transient activation of the PI3K pathway, we used a Pten inhibitor, dipotassium bisperoxo(5-hydroxypyridine-2-carboxyl)oxovanadate [bpV(HOpic)],[25] during the process of iPSC generation (from day 0 to 10 after transduction) (**Figure 2b**). The bpV(HOpic) concentration was considered optimal at 100 nmol/l, which was determined by analyzing the activation status of Akt in MEFs by western blotting (**Supplementary Figure S1** and **Supplementary Materials and Methods**). MEFs cultured in medium containing 100 nmol/l bpV(HOpic) were transduced with OKSM, resulting in generation of ESC-like colonies (bpV-iPSCs) on day 14 after transduction (**Figure 2b,e**, left panel). After isolation of these ESC-like colonies on day 14 after transduction, eight bpV-iPSC lines were established and expanded in conventional ESC medium on SNL feeders and then characterized further (**Supplementary Table S1**). Reverse transcription PCR showed that all of the bpV-iPSC lines examined (8/8) expressed ESC markers such as endogenous *Oct3/4*, *Sox2*, and *Nanog* (**Figure 2d**). In addition, bpV-iPSC lines were positive for AP activity and SSEA1 staining (**Figure 2e**, middle and right panels, respectively). It should be noted that the efficiency of iPSC generation from OKSM-transduced MEFs in the presence of bpV(HOpic) was much higher than that from the untreated control (353±42 versus 189±32; **Figure 2c**, left panel). Furthermore, inhibition of the PI3K pathway by LY294002,[26] a reversible inhibitor of all classes of PI3Ks, resulted in a sharp decrease of the efficiency of iPSC generation (20±11; **Figure 2c**, left panel). Similar results were obtained when OKS were transduced in the presence

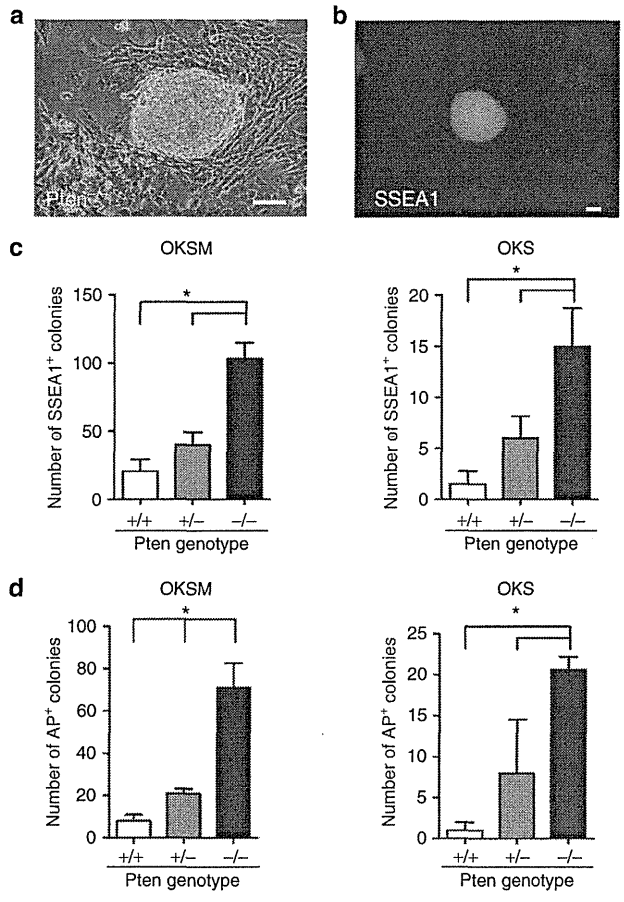

Figure 1 Loss of Pten promotes reprogramming of MEFs into iPSCs. (**a**) Representative image of an iPSC colony derived from Pten$^{-/-}$ MEFs by transduction of mouse OKSM. Scale bar = 100 μm. (**b**) Immunocytochemical staining of SSEA1 on iPSCs induced by transduction of OKSM into Pten$^{-/-}$ MEFs. Scale bar = 0.2 mm. (**c**) Counts of SSEA1$^+$ colonies. A total of 5,000 (OKSM) or 50,000 (OKS) retrovirally transduced MEFs with Pten$^{+/+}$, Pten$^{+/-}$, or Pten$^{-/-}$ genotypes were transferred onto feeders on day 4 after transduction. SSEA1$^+$ colonies were counted on day 14 (OKSM, left) and day 28 (OKS, right) after transduction. Data are the mean ± SD (n = 3), *P < 0.05 versus wild type. (**d**) Counts of AP$^+$ colonies derived from single cells. A total of 100 MEFs (OKSM or OKS) with Pten$^{+/+}$, Pten$^{+/-}$, or Pten$^{-/-}$ genotypes were transferred onto feeders on day 4 after transduction. AP$^+$ colonies generated from Pten$^{+/+}$, Pten$^{+/-}$, or Pten$^{-/-}$ MEFs transduced with OKSM (left) or OKS (right) were counted on day 12 (OKSM) and day 28 (OKS) after transduction. Data are the mean ± SD (n = 3 or more), *P < 0.05 versus wild type. iPSC, induced pluripotent stem cell; MEF, mouse embryonic fibroblast.

of bpV(HOpic) (89±11 versus 60±5; **Figure 2c**, right panel). Moreover, the emergence of SSEA1$^+$ colonies from MEFs transduced with OKSM was enhanced by bpV(HOpic) treatment (n = 3, P < 0.05; **Supplementary Figure S2**).

These results were further confirmed by experiments using MEFs carrying the green fluorescent protein (GFP) gene under the control of the *Nanog* promoter (*Nanog*-GFP MEFs).[12] We found that transient treatment with bpV(HOpic) significantly increased the number of *Nanog*-GFP$^+$ colonies from MEFs transduced with OKSM or OKS under a feeder-free condition (n > 3, P < 0.05; **Figure 3a**). These results strongly indicated that inhibition of Pten promoted the efficiency of iPSC generation by transduction of OKSM or OKS.

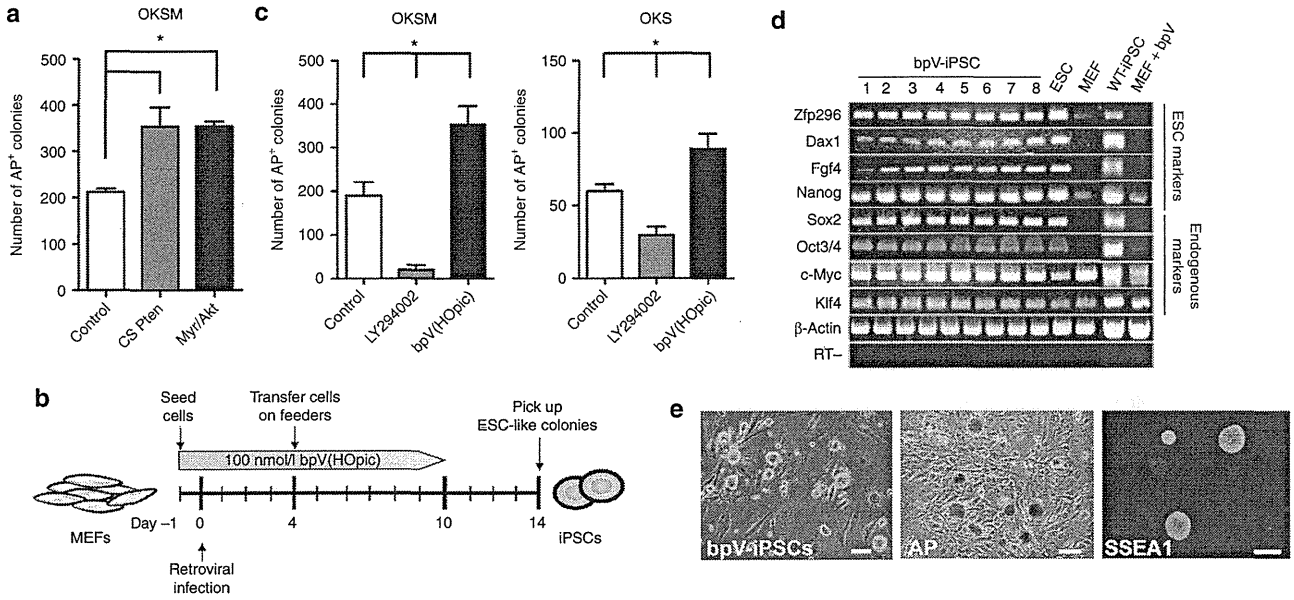

Figure 2 Activation of the PI3K-Akt pathway enhances iPSC generation. (**a**) Counts of AP+ colonies formed by transduction of OKSM combined with the dominant-negative form of Pten (CS-Pten) or activated form of Akt (myr-Akt) into MEFs. Wild-type MEFs (1×10^5) were transduced with OKSM (control, left), OKSM+CS-Pten (middle), or OKSM+myr-Akt (right). Cells (5,000) were transferred onto SNL feeders on day 4 after transduction and cultured in ESC medium. AP+ colonies were counted on day 14 after transduction. Data are the mean ± SD ($n = 3$), $^*P < 0.05$ versus control. (**b**) Experimental scheme for iPSC generation. MEFs (1×10^5) were infected with retroviruses carrying OKSM on day 0. Cells (5,000) were transferred onto SNL feeders on day 4 after transduction and cultured in ESC medium containing 100 nmol/l bpV(HOpic). Colonies were collected based on ESC-like morphology on day 14 after transduction. The Pten inhibitor bpV(HOpic) was added from day –1 to 10. (**c**) Counts of AP+ colonies formed by transduction of OKSM or OKS into MEFs in the presence of LY294002 or bpV(HOpic). A total of 5,000 (OKSM) or 50,000 (OKS) retrovirally transduced MEFs were transferred onto SNL feeders on day 4 after transduction and then cultured in the presence of 100 nmol/l bpV(HOpic) or 5 μmol/l LY294002 for 10 (OKSM) or 28 days (OKS). AP+ colonies were counted on day 10 (OKSM, left panel) and day 28 (OKS, right panel). AP+ colonies generated without drugs were used as controls. Data are the mean ± SD ($n = 3$), $^*P < 0.05$ versus controls. (**d**) Characteristics of bpV-iPSCs *in vitro*. The expression of ESC marker genes in bpV-iPSCs (OKSM) was examined by RT PCR (bpV-iPSC clones 1–8). Mouse β-actin was used as a loading control. The RT (–) control is shown at the bottom. (**e**) Representative images of bpV-iPSC colonies (left panel), AP staining (middle panel), and SSEA1 staining (right panel). Scale bars = 100 μm. ESC, embryonic stem cell; iPSC, induced pluripotent stem cell; MEF, mouse embryonic fibroblast; RT, reverse transcription.

It has been reported that the use of PS48, a small molecule activator of 3′-phosphoinositide–dependent kinase-1 (PDK1) that is involved in the PI3K pathway, can enhance the reprogramming efficiency for iPSC generation from human cells.[27] We therefore examined whether bpV(HOpic) or PS48 could further enhance the reprogramming efficiency. We found that a significantly higher number of AP+ colonies were formed from bpV(HOpic)-treated MEFs compared with that from PS48-treated MEFs ($n = 3$, $P < 0.05$; **Supplementary Figure S3**), indicating that inhibition of Pten by bpV(HOpic) might be a better approach than activation of PDK1 by PS48 for the enhancement of reprogramming.

To exclude the possibility that nonspecific effects of bpV(HOpic) had affected the iPSC generation, we also tested other specific Pten inhibitors such as SF1670 and bpV(Phen). As a result, the number of AP+ colonies appeared to significantly increase on day 10 after transduction in the presence of SF1670 or bpV(Phen) (**Supplementary Figure S4**).

It has been reported that various kinds of chemicals and supplements, such as histone deacetylase inhibitors, valproic acid (VPA), MAPK/ERK kinase inhibitors + glycogen synthase kinase 3β (GSK3β) inhibitors (2i), and vitamin C (Vc), enhance the reprogramming efficiency of somatic cells into iPSCs.[6,28–30] Therefore, various combinations of bpV(HOpic) were tested with these compounds, such as bpV(HOpic)+Vc, bpV(HOpic)+2i, and bpV(HOpic)+VPA. We found that combined use of bpV(HOpic) with each compound significantly increased the number of AP+ or *Nanog*-GFP+ colonies generated from OKSM-transduced MEFs ($n = 3$, $P < 0.05$; **Supplementary Figure S5** and **Supplementary Materials and Methods**). In particular, bpV(HOpic)+VPA strongly enhanced the reprogramming efficiency by more than fourfold compared with that of bpV(HOpic) alone (12±4 versus 48±7; **Supplementary Figure S5**).

Next, we examined the characteristics of bpV-iPSCs. Bisulfite genomic sequencing analyses were performed to examine epigenetic modification of pluripotency-associated promoter regions such as *Nanog* and *Oct3/4* genes.[1,2,12,31] The promoters of *Nanog* and *Oct3/4* genes in OKSM- and OKS-transduced bpV-iPSCs were less methylated than those in MEFs, which was similar to those in ESCs (**Figure 3b** and **Supplementary Figure S6**), suggesting that similar DNA methylation patterns of pluripotency genes, such as Nanog and Oct3/4, stably maintained the undifferentiated state of bpV-iPSCs.

In addition, karyotype analyses showed that the chromosomal status of bpV-iPSCs was normal over 15 passages (**Supplementary Figure S7**), indicating that transient activation of the PI3K pathway by a Pten inhibitor, bpV(HOpic), did not affect chromosomal stability in the process of reprogramming.

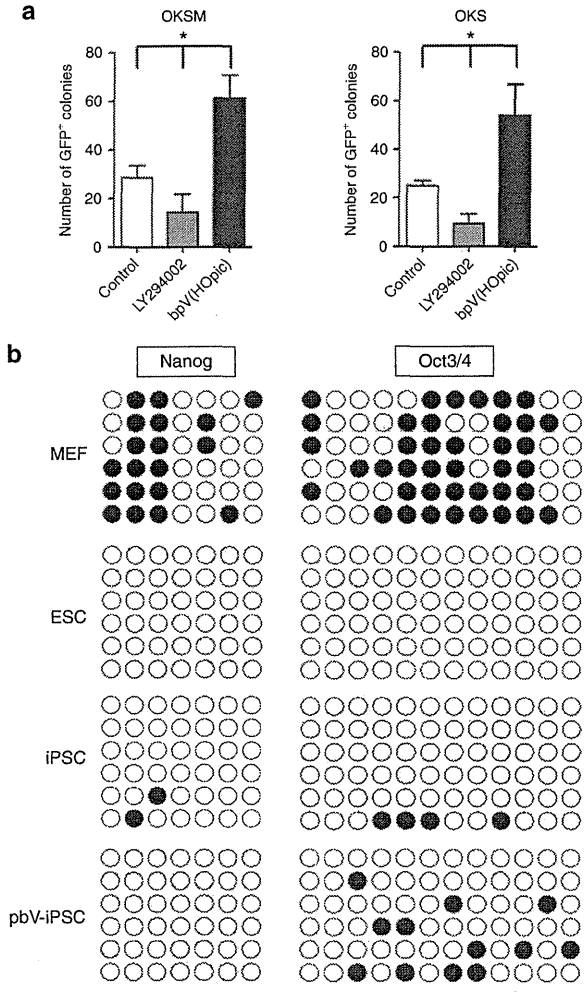

Figure 3 Addition of bpV(HOpic) improves the reprogramming of *Nanog*-GFP MEFs by OKSM or OKS. (**a**) Counts of *Nanog*-GFP$^+$ colonies formed by transduction of OKSM or OKS into MEFs in the presence of LY294002 or bpV(HOpic). *Nanog*-GFP MEFs were retrovirally transduced with OKSM (left panel) or OKS (right panel) and then cultured in the presence of 5 μmol/l LY294002 or 100 nmol/l bpV(HOpic) for 9 days (from day 5 to 14 after transduction, left panel) or 33 days (from day 5 to 38 after transduction, right panel). The number of GFP$^+$ colonies was counted by observation under an immunofluorescence microscope. Data are the mean ± SD ($n = 12$ for LY294002- or bpV(HOpic)-treated groups and $n = 6$ for the control group), $^*P < 0.05$. (**b**) DNA methylation analysis of the promoter regions for endogenous *Nanog* and *Oct3/4* genes. Genomic DNA from wild-type MEFs, mouse ESCs, wild-type iPSCs, and bpV-iPSCs (OKSM) were analyzed by bisulfite sequencing. Open and closed circles indicate unmethylated and methylated CpG islands, respectively. ESC, embryonic stem cell; iPSC, induced pluripotent stem cell; MEF, mouse embryonic fibroblast.

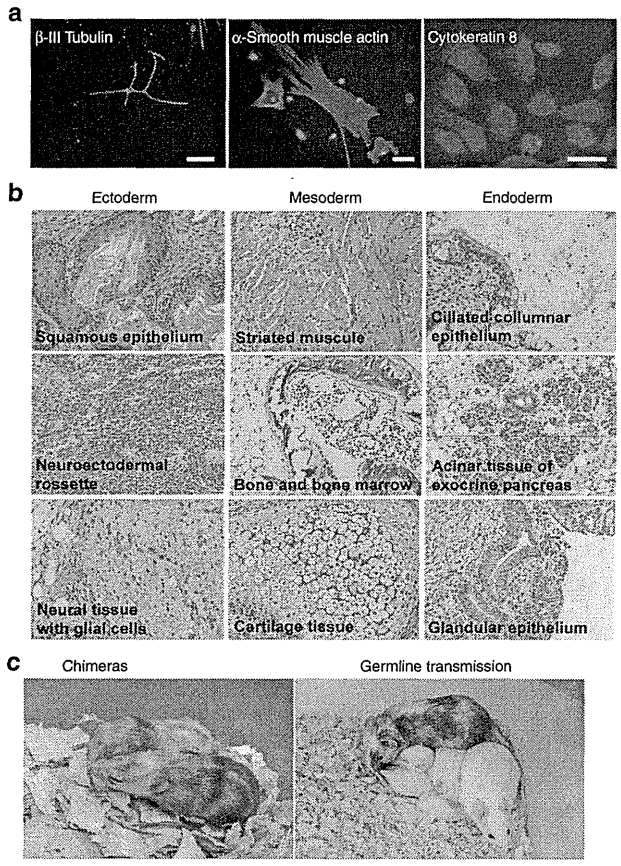

Figure 4 Pluripotency of bpV-iPSCs. (**a**) *In vitro* differentiation ability of bpV-iPSCs. After EB formation for 7 days, EBs were transferred onto 0.1% gelatin-coated dishes, cultured for another 6 days, fixed, and then processed for immunocytochemistry using antibodies against β-III tubulin (ectoderm marker, left panel), α-smooth muscle actin (mesoderm marker, middle panel), and cytokeratin 8 (endoderm marker, right panel). Scale bars = 50 μm. (**b**) *In vivo* differentiation ability of bpV-iPSCs. Hematoxylin-eosin staining of tissue sections showing teratomas composed of mature tissues derived from the three embryonic germ layers. Magnification ×200. (**c**) Contribution of bpV-iPSCs to chimeric mice. Injection of bpV-iPSCs derived from ICR mice into C57BL/6 blastocysts led to the generation of chimeric mice (left panel). Offspring (chimera male × ICR female) were white, indicating germline transmission of bpV-iPSCs (right panel). iPSC, induced pluripotent stem cell.

We next examined *in vitro* and *in vivo* differentiation potentials of bpV-iPSCs. bpV-iPSC differentiation was induced by embryoid body (EB) formation *in vitro*. Immunocytochemical analysis revealed that EB-formed cells expressed lineage markers of the ectoderm (β-III tubulin), mesoderm (α-smooth muscle actin), and endoderm (cytokeratin 8) (**Figure 4a**). We then performed a teratoma formation assay *in vivo*. One-million bpV-iPSCs were injected into the testes and backs of SCID mice. At 4–5 weeks after injection, we observed tumor formation. Histological analyses by hematoxylin-eosin staining showed that the tumors contained various derivatives of the three germ layers, indicating development of a well-differentiated teratoma (**Figure 4b**). Moreover, bpV-iPSCs contributed to somatic tissue formation in chimeric mice and showed a germline transmission capability (**Figure 4c**). These results strongly indicated that bpV-iPSCs possessed pluripotency *in vitro* and *in vivo*.

Next, we attempted to elucidate the mechanisms that promoted iPSC generation by the Pten inhibitor. We first examined the effect of bpV(HOpic) on the reprogramming time window by transduction of OKSM or OKS into *Nanog*-GFP MEFs. We found that the reprogramming time window was not affected by the addition of bpV(HOpic), although the number of GFP$^+$ cells was increased on around day 10 (OKSM) and day 15 (OKS) after transduction (**Figure 5a**).

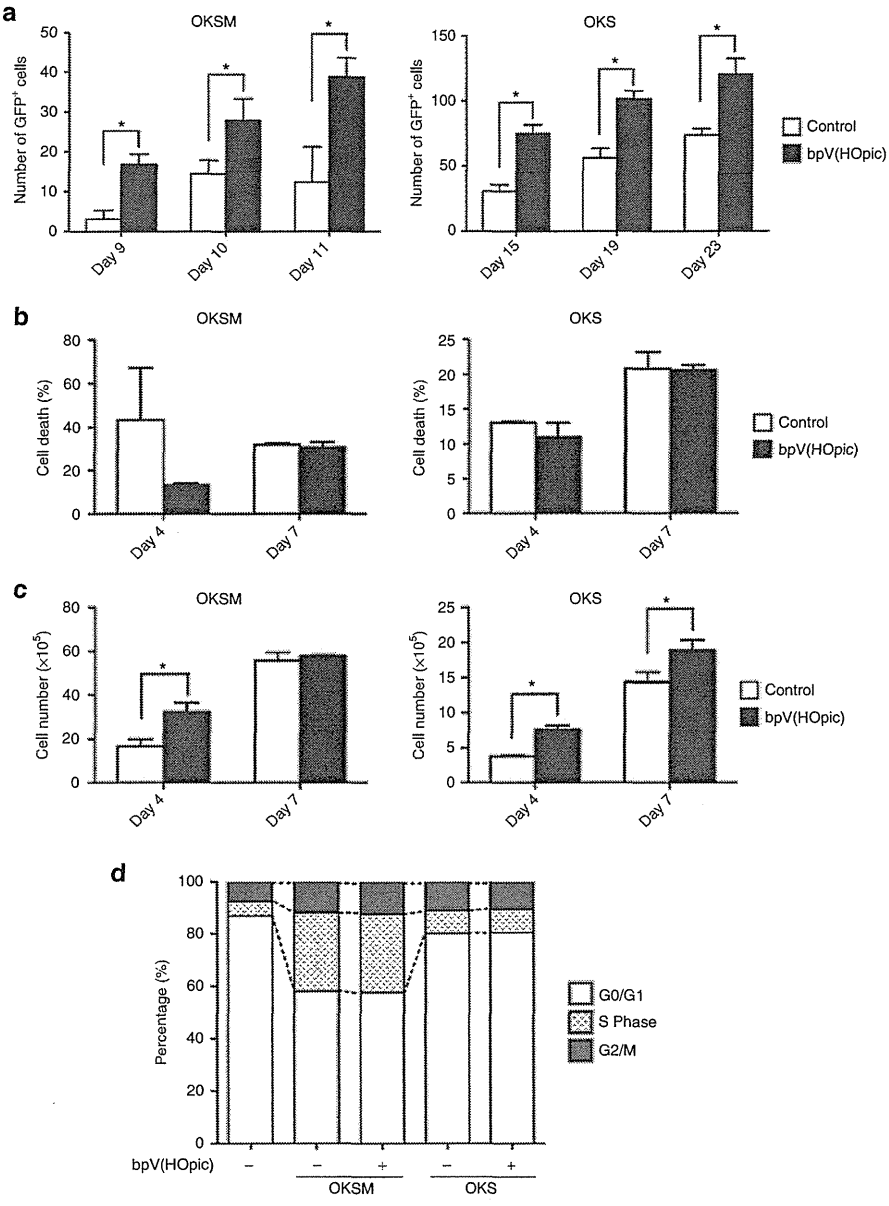

Figure 5 Effects of bpV(HOpic) on survival, proliferation, and reprogramming of MEFs. (**a**) Promotion of reprogramming by bpV(HOpic). *Nanog*-GFP MEFs were retrovirally transduced with OKSM (upper panel) or OKS (lower panel) and then cultured in the presence (black bar) or absence (white bar) of bpV(HOpic). The number of GFP+ cells was counted by observation under an immunofluorescence microscope at the indicated time points after transduction. Data are the mean ± SD ($n = 3$), $^*P < 0.05$. (**b**) Analysis of cell death. OKSM- (left panel) or OKS- (right panel) transduced MEFs were cultured with or without 100 nmol/l bpV(HOpic) for 4 or 7 days. The annexin V+ cell population was analyzed by flow cytometry. Data are the mean ± SD ($n = 3$). (**c**) Effects of bpV(HOpic) on cell proliferation. The number of OKSM- (left panel) or OKS- (right panel) transduced MEFs cultured with or without 100 nmol/l bpV(HOpic) for 4 or 7 days was counted. Data are the mean ± SD ($n = 3$), $^*P < 0.05$. (**d**) Cell cycle analysis. OKSM- or OKS-transduced MEFs were cultured in the presence of 100 nmol/l bpV(HOpic) for 4 days, and then a BrdU assay was performed. MEFs and OKSM- or OKS-transduced MEFs without bpV(HOpic) treatment were used as controls. Data are the mean ± SD ($n = 3$). GFP, green fluorescent protein; MEF, mouse embryonic fibroblast.

To further address how the efficiency of iPSC generation was enhanced by Pten inhibition, we examined cell death, cell cycle distribution, and proliferation affected by bpV(HOpic). Cell survival of OKSM- and OKS-transduced MEFs treated with bpV(HOpic) in the process of reprogramming was assessed using annexin V staining. We did not observe any significant increase or decrease in cell death induced by bpV(HOpic) at the indicated time points (**Figure 5b**), although cell death on day 4 after transduction tended to be inhibited in the presence of bpV(HOpic). However, we found that the proliferation rate of OKSM- and OKS-transduced MEFs treated with bpV(HOpic) was slightly higher than that of the untreated control (**Figure 5c**), although the data from OKSM-transduced MEFs on day 7 after transduction showed no effect on proliferation induced by bpV(HOpic). These data indicated that

bpV(HOpic) treatment slightly promoted cell proliferation, particularly during the early phase of reprogramming of OKSM- and OKS-transduced MEFs. However, the cell cycle distribution was not changed significantly (**Figure 5d**). These results indicated that the enhancement of iPSC generation by Pten inhibition was associated with slightly accelerated cell proliferation during the early phase of reprogramming.

DISCUSSION

It is known that the efficiency of iPSC generation by retroviral transfer of reprogramming factors into MEFs is ~0.1–1%.[1–4,6,7] In this study, we have developed a novel method that enhances the reprogramming efficiency of OKSM-transduced mouse somatic cells by transient activation of the PI3K pathway using a Pten inhibitor, bpV(HOpic). The efficiency of AP^+ cell generation from OKSM-transduced MEFs by the addition of bpV(HOpic) was ~7% (**Figure 2c**, left panel). This high proportion of AP^+ cells was surprising, but there was a possibility that insufficiently reprogrammed cells were included in the AP^+ population. Therefore, we also examined the efficiency of $SSEA1^+$ cell generation from MEFs. The proportion of $SSEA1^+$ cells generated from OKSM-transduced MEFs treated with bpV(HOpic) was ~3% ($n = 3$, $P < 0.05$; **Supplementary Figure S2**), strongly suggesting the ability of bpV(HOpic) to enhance iPSC generation. It should also be noted that combined use of bpV(HOpic) with VPA further improved iPSC generation (**Supplementary Figure S5b**).

The mechanisms of bpV(HOpic) treatment, which increase the efficiency of iPSC generation, are considered to be crucial. We have shown that treatment with LY294002 from day 0 to 10 after OKSM transduction inhibited the efficiency of iPSC generation (**Figure 2c**), whereas expression of the activated form of Akt (myr-Akt)-enhanced iPSC generation (**Figure 2a**). Thus, it is conceivable that activation of the PI3K-Akt pathway due to inhibition of Pten by bpV(HOpic) at least in part plays a role in the reprogramming process.

Several molecules downstream of the PI3K-Akt pathway are responsible for critical biological phenomena such as self-renewal, and cell survival and proliferation. It has been reported that *c-Myc* and its downstream target, cyclin D, are activated by the PI3K-Akt pathway,[32] which leads to acceleration of the cell cycle. Another report has described that Akt inhibits cell cycle inhibitory molecules, p21 and p27.[8,33] This evidence indicates that activation of the PI3K-Akt pathway promotes cell proliferation. Indeed, MEFs treated with bpV(HOpic) showed a slightly higher rate of proliferation (**Figure 5b**). Previous reports have described that promotion of cell proliferation results in the enhancement of iPSC generation.[34] Thus, the acceleration of cell proliferation caused by the treatment with bpV(HOpic) may be associated with the activation of cell cycle molecules, which leads to the elevation of the efficiency of iPSC generation from somatic cells.

Several reports have shown that GSK3β is a key regulator of cellular fate and a participant in differentiation events during embryonic development through the Wnt/GSK3β/β-catenin signaling pathway.[35] Phosphorylation of GSK3β by Akt allows translocation of β-catenin into the nucleus, which activates transcription factors such as *c-Myc* and *Nanog* and promotes reprogramming.[29,36] Therefore, the use of bpV(HOpic) might inhibit GSK3β through activation of the PI3K-Akt pathway, resulting in the enhancement of iPSC generation.

Recently, treatment with 0.3 μmol/l LY294002, a PI3K pathway inhibitor, from day 1 to 3 after OKSM transduction was shown to enhance the efficiency of iPSC generation from MEFs.[37] However, in our study, treatment with 5 μmol/l LY294002 from day 0 to 10 after OKSM transduction inhibited the efficiency of iPSC generation (**Figure 2c**). The discrepancy between these data might be due to the difference in drug concentrations and/or the duration of drug treatment used for iPSC generation.

It has been reported that the efficiency of reprogramming is enhanced by increased cell proliferation and survival by inhibition of the p53-p21 pathway and *Ink4a/Arf* locus.[8,33,34,38–42] Indeed, use of the p53 inhibitor pifithrin-α hydrobromide (PFTα) tended to show a higher reprogramming efficiency (**Supplementary Figure S8**). However, p53 was slightly accumulated in OKSM-transduced MEFs treated with bpV(HOpic) (**Supplementary Figure S9**), indicating that promotion of iPSC generation by bpV(HOpic) was not due to reduced p53 protein levels. Further investigation is needed to reveal the significance of slight p53 stabilization in OKSM-transduced MEFs treated with bpV(HOpic).

Interestingly, for cell proliferation, previous reports have shown that mitochondrial oxidation is generally used in differentiated somatic cells, whereas glycolysis is mainly used in pluripotent cells.[27,43] In addition, it has been shown that modulation of cell metabolism from mitochondrial oxidation to glycolysis plays an important role in the process of iPSC generation.[27,43,44] Because PI3K signaling is known to be a potent regulator of cellular metabolism,[45] the possibility that inhibition of Pten by bpV(HOpic) induces a change of metabolic pathways from mitochondrial oxidation to glycolysis should also be carefully examined in the future.

Because continuous activation of the PI3K pathway causes transformation of cells,[46] bpV(HOpic) treatment may cause the emergence of cancer cells. However, iPSCs generated in the presence of bpV(HOpic) could be readily and stably expanded over a long term under conventional ESC culture conditions (>15 passages) and exhibited a normal karyotype (**Supplementary Figure S7**). Furthermore, they could directly differentiate into the three germ layers *in vitro* and formed teratomas *in vivo*. In mice, injection of these bpV-iPSCs into C57BL/6 host blastocysts resulted in the generation of healthy chimeric mice showing a germline transmission capability (**Figure 4**). Out of 11 chimeric mice aged over 1 year, nine mice did not survive owing to unknown reasons, and only one mouse formed a teratoma in the left leg (data not shown). Teratoma formation in a bpV-iPSC chimeric mouse might be influenced by reactivation of reprogramming factors or transient activation of the PI3K pathway in the process of reprogramming. In addition, some of the bpV-iPSCs injected into blastocysts might remain in an undifferentiated state. These possibilities need to be carefully considered when iPSC-based cell replacement therapies are conducted for regenerative medicine in the future.

MATERIALS AND METHODS

Plasmids. pMXs-based retroviral vectors for mouse *Oct3/4*, *Klf4*, *Sox2*, and c-*Myc* were obtained from Addgene (Cambridge, MA).[47] pMXs vectors encoding a mutant derivative of Pten containing a Cys-124 to serine

substitution (*CS-Pten*),[22] *myr-Akt*, or *GFP* genes were gifts from Akira Suzuki (Kyushu University, Fukuoka, Japan).

Cell culture. PLAT-E cells for production of retroviruses were kindly provided by Dr. Toshio Kitamura (Tokyo University, Tokyo, Japan) and maintained in Dulbecco's modified Eagle's medium (DMEM; Invitrogen, Carlsbad, CA) containing 10% fetal bovine serum (FBS; Invitrogen), 1 mg/ml puromycin (InvivoGen, San Diego, CA), and 10 μg/ml blasticidin S (InvivoGen).[48] MEFs were isolated from pregnant mice at gestational day 12 (Crlj: CD1, Charles River, Japan; *Nanog*-GFP Mouse, Rikken, Japan) and expanded in fibroblast medium consisting of DMEM/10% FBS with 1% antibiotic-antimycotic mixed stock solution (Nacalai Tesque, Kyoto, Japan). Pten-deficient MEFs were kindly provided from Dr. Akira Suzuki (Kyushu University, Fukuoka, Japan).[19] SNL feeders and MEFs were cultured in DMEM/10% FBS with antibiotics on 0.1% gelatin-coated dishes at 37 °C with 5% CO_2. SNL feeders were treated with 12 μg/ml MMC (Kyowa Hakko Kirin, Tokyo, Japan) for around 2 hours before coculture with iPSCs. Mouse iPSCs were cultured on gelatin-coated plates with MMC-treated SNLs in mouse ESC medium consisting of knockout DMEM containing 1000 U/ml leukemia inhibitory factor (Wako, Osaka, Japan), 2 mmol/l L-glutamine (Nacalai Tesque), 10% FBS, 0.1 mmol/l 2-mercaptoethanol (Sigma-Aldrich, St Louis, MO), 1% nonessential amino acids (Invitrogen), and 50 IU/ml penicillin and 50 mg/ml streptomycin mixed solution (Nacalai Tesque).

Retrovirus production and iPSC generation. For retroviral production, PLAT-E cells were seeded at 3.3×10^6 cells per 100 mm dish. The following day, 9 μg pMXs-based retroviral vectors for expression of GFP, *Oct3/4*, *Klf4*, *Sox2*, or *c-Myc* were individually introduced into PLAT-E cells using FuGENE 6 transfection reagent (Roche Diagnostics, Indianapolis, IN). After 24 hours, the medium was replaced with 10 ml DMEM/10% FBS, and the supernatant was collected on the following day. On day 0, equal volumes of supernatants from PLAT-E cell cultures containing retroviruses carrying each factor were mixed, and then 1×10^5 (OKSM) – 1×10^6 (OKS) ICR-MEFs or 8×10^4 (OKSM) – 1×10^6 (OKS) Nanog-GFP MEFs were incubated with the mixture. At 4 days after infection, the cells were transferred onto MMC-treated SNL feeders and cultured in ESC medium. Using 35-mm dishes, 5,000 OKSM-transduced and 50,000 OKS-transduced cells were transferred onto SNL feeders. AP^+ and $SSEA1^+$ colonies were examined on day 14 for OKSM-transduced cells, and on day 28 for OKS-transduced cells. To examine the efficiency of iPSC generation from single cell population, 100 of OKSM-transduced cells or 100 of OKS-transduced cells were transferred onto MMC-treated SNL feeders on day 4 after transduction, and their AP activity was examined on days 14 (OKSM) and 28 (OKS), respectively.

Regulation of the PI3K-Akt pathway. To activate the PI3K-Akt pathway, MEFs were retrovirally transduced with a dominant-negative mutant type of Pten (CS-Pten)[22] or activated form of myristoylated Akt (myr-Akt).[23] Moreover, to activate the PI3K-Akt pathway with the Pten inhibitor, MEFs were treated with bpV(HOpic) (100 nmol/l; Calbiochem, Darmstadt, Germany), bpV(Phen) (100 nmol/l; Calbiochem), SF1670 (500 nmol/l; Cellagen Technology, San Diego, CA), or PS48 (5 μmol/l; Wako). Then, to inhibit the PI3K-Akt pathway, cells were treated with LY294002 (5 μmol/l; Santa Cruz Biotechnology, Heidelberg, Germany).

AP staining. AP staining was performed using an Alkaline Phosphatase Kit (Sigma-Aldrich). Colonies grown in 35-mm dishes were fixed in a fixative solution for 30 seconds at room temperature and then washed twice with deionized water for 45 seconds. Fixed cells were incubated with the AP staining solution while protected from light for 1 hour at room temperature and then washed twice with deionized water for 2 minutes. The samples were then observed by optical microscopy (Axiovert 135; ZEISS, Deutschland, Germany).

Immunocytochemical staining. Cells were fixed with 4% paraformaldehyde in phosphate-buffered saline (PBS) for 30 minutes and then washed extensively with PBS. The cells were then permeabilized with 0.3% Triton X-100 in PBS for 5 minutes, followed by blocking with 3% bovine albumin serum in PBS. Staining was carried out by incubation with an anti-SSEA1 antibody (Santa Cruz Biotechnology) overnight at 4 °C. After extensive washing, an antimouse Alexa546 antibody (Invitrogen) was applied for 1 hour at room temperature, and then the cells were counterstained with 4,6-diamindino-2-phenylindole-2 (Invitrogen). Images were obtained by immunofluorescence microscopy (BZ-9000, KEYENCE, Osaka, Japan).

Reverse transcription PCR. Total RNA was extracted from cultured cells using an RNeasy kit (Qiagen, Courtaboeuf, France), and cDNA was synthesized using a reverse transcription system (Invitrogen). PCR was performed using KOD FX DNA polymerase (Toyobo, Tokyo, Japan) according to the manufacturer's instructions. Primer sequences are described in **Supplementary Tables S2** and **S3**. PCR products were size fractionated on 1% agarose gels. β-actin was used as a loading control.

Bisulfite sequencing and karyotype analysis. Genomic DNA from mouse ESCs, MEFs, and bpV-iPSCs was extracted with a DNeasy Blood & Tissue Kit (Qiagen) and then treated with sodium bisulfite using a BisulFast DNA Modification Kit (Toyobo). Treated DNA was purified using an EZ kit (Zymo Research, Orange, CA). Then, *Nanog* and *Oct3/4* gene promoter regions[49] were amplified by PCR using primers shown in **Supplementary Table S4**. PCR products were inserted into a pGEM-T easy vector (Promega, Madison, WI) and then sequenced using M13 primers. Karyotype analysis was performed at the ICLAS Monitoring Center, Central Institute for Experimental Animals.

Spontaneous differentiation* in vitro *and immunocytochemistry. The pluripotency of bpV-iPSCs was assessed by an *in vitro* differentiation assay. Briefly, single cells were harvested by trypsinization, and 1×10^6 cells were cultured on low adhesion plates in mouse ESC medium without leukemia inhibitory factor. Half medium volumes were exchanged every day, and EBs were allowed to grow for 6–7 days in suspension. Then, EBs were trypsinized and replated onto 0.1% gelatin-coated dishes and cultured for another 7 days (ectoderm) or 14 days (endoderm and mesoderm). Spontaneous differentiation was examined by immunocytochemistry using antibodies against cytokeratin 8 (Invitrogen), α-smooth muscle actin (Sigma, St Louis, MO), and β-III tubulin (Sigma). The samples were observed by immunofluorescence microscopy (BZ-9000).

Teratoma formation assay. The bpV-iPSCs (1×10^6) were resuspended in 50 μl PBS and then injected into the testis or back of SCID mice (Charles River Laboratories). At 4–8 weeks after injection, formed tumors were removed and fixed in 4% paraformaldehyde/PBS overnight at 4 °C. Tumor tissues were embedded in paraffin. Tissue blocks were sectioned at 3 μm and stained with hematoxylin-eosin. All animal experiments were approved by the Animal Committees at Kyushu University and Kumamoto University, Japan.

Generation of chimeric mice. To generate chimeric mice derived from bpV-iPSCs, C57BL/6 host blastocysts injected with bpV-iPSCs were transplanted into the uteri of surrogate ICR mice. Detailed protocols have been described before.[50]

Proliferation and cell death analyses. OKSM- or OKS-transduced MEFs (1×10^5) were cultured in DMEM/10% FBS with or without bpV(HOpic). On days 4 and 7, cells were harvested and counted with a TC10 automated cell counter (Bio-Rad, Hercules, CA) to determine the cell number. The cells were then stained with annexin V-APC (BD Pharmingen, San Diego, CA), and the population of annexin V^+ dead cells was analyzed by flow cytometry (FACS Verse; BD Biosciences, San Jose, CA).

BrdU assay. The BrdU incorporation assay was performed with BrdU FLOW Kits according to the manufacturer's instructions (BD Pharmingen). Briefly, OKSM- or OKS-transduced MEFs were cultured in the presence

of 10 μmol/l BrdU-labeling reagent (BD Pharmingen) for 1 hour. Then, the cells were harvested and dissociated into single cells with a trypsin/EDTA solution (Nacalai Tesque). Single cells were fixed, permeabilized, and stained with antibodies against BrdU and 7-AAD, and then samples were analyzed by flow cytometry (FACS Verse).

Statistical analyses. Data were shown as the mean ± SD and analyzed for statistical significance by GraphPad Prism version 5.0d (GraphPad Software, San Diego, CA). For comparisons between groups, the data were analyzed using a *t*-test or one-way analysis of variance with Tukey's multiple comparison. A value of $P < 0.05$ was considered as significant.

SUPPLEMENTARY MATERIAL

Figure S1. Effect of Pten inhibitor, bpV(HOpic) on Akt activation.
Figure S2. Number of SSEA1$^+$ colonies generated from MEFs in the presence of bpV(HOpic).
Figure S3. Number of AP$^+$ colonies generated in the presence of PDK1 activator, PS48, or Pten inhibitor, bpV(HOpic).
Figure S4. Effects of various Pten inhibitors on iPSC generation.
Figure S5. Enhanced efficiency of iPSC generation by combined use of bpV(HOpic) with various compounds.
Figure S6. DNA methylation analysis of the promoter regions of endogenous *Nanog* and *Oct3/4* genes in OKS-transduced iPSCs.
Figure S7. Karyotype analysis of OKSM-transduced bpV-iPSCs.
Figure S8. Effects of p53 and Pten inhibitors on iPSC generation.
Figure S9. p53 expression in MEFs treated with bpV(HOpic).
Table S1. Summary of established bpV-iPSC cell lines.
Table S2. Primers used for RT-PCR.
Table S3. Endogenous primers used for RT-PCR.
Table S4. Primers used for bisulfite sequencing.
Materials and Methods.

ACKNOWLEDGMENTS

The authors thank Ken-ichi Yamamura (Scientific Support Programs for Cancer Research Grant-in-Aid for Scientific Research on Innovative Areas, Kumamoto University, Japan), and Masato Tanaka and Kaori Nagatoshi for their help to establish chimeras. They also thank Michiko Ushijima for administrative assistance, Atsushi Takahashi and the members of Kenzaburo Tani's laboratory for providing constructive criticism and technical assistance, and Peng Xiong (Kyushu University) for his help in performing statistical analysis. They also thank Hiroyuki Sasaki (Kyushu University) for helpful discussions and providing bisulfite PCR primers for *Nanog*. This work was partly performed in the Cooperative Research Project Program of the Medical Institute of Bioregulation, Kyushu University, the Research Support Center (Graduate School of Medical Sciences, Kyushu University) and Laboratory for Technical Support (Medical Institute of Bioregulation, Kyushu University) for technical assistance. This work was supported by grants from the Project for Realization of Regenerative Medicine (K.T., 08008010) and KAKENHI (T.M., 23590465) from the Ministry of Education, Culture, Sports, Science, and Technology (MEXT), Japan. The authors declare no conflict of interest.

REFERENCES

1. Takahashi, K and Yamanaka, S (2006). Induction of pluripotent stem cells from mouse embryonic and adult fibroblast cultures by defined factors. *Cell* **126**: 663–676.
2. Takahashi, K, Tanabe, K, Ohnuki, M, Narita, M, Ichisaka, T, Tomoda, K *et al.* (2007). Induction of pluripotent stem cells from adult human fibroblasts by defined factors. *Cell* **131**: 861–872.
3. Yu, J, Vodyanik, MA, Smuga-Otto, K, Antosiewicz-Bourget, J, Frane, JL, Tian, S *et al.* (2007). Induced pluripotent stem cell lines derived from human somatic cells. *Science* **318**: 1917–1920.
4. Nakagawa, M, Koyanagi, M, Tanabe, K, Takahashi, K, Ichisaka, T, Aoi, T *et al.* (2008). Generation of induced pluripotent stem cells without Myc from mouse and human fibroblasts. *Nat Biotechnol* **26**: 101–106.
5. Wernig, M, Meissner, A, Foreman, R, Brambrink, T, Ku, M, Hochedlinger, K *et al.* (2007). *In vitro* reprogramming of fibroblasts into a pluripotent ES-cell-like state. *Nature* **448**: 318–324.
6. Esteban, MA, Wang, T, Qin, B, Yang, J, Qin, D, Cai, J *et al.* (2010). Vitamin C enhances the generation of mouse and human induced pluripotent stem cells. *Cell Stem Cell* **6**: 71–79.
7. Stadtfeld, M and Hochedlinger, K (2010). Induced pluripotency: history, mechanisms, and applications. *Genes Dev* **24**: 2239–2263.
8. Hanna, J, Saha, K, Pando, B, van Zon, J, Lengner, CJ, Creyghton, MP *et al.* (2009). Direct cell reprogramming is a stochastic process amenable to acceleration. *Nature* **462**: 595–601.
9. Storm, MP, Bone, HK, Beck, CG, Bourillot, PY, Schreiber, V, Damiano, T *et al.* (2007). Regulation of Nanog expression by phosphoinositide 3-kinase-dependent signaling in murine embryonic stem cells. *J Biol Chem* **282**: 6265–6273.
10. Jeong, CH, Cho, YY, Kim, MO, Kim, SH, Cho, EJ, Lee, SY *et al.* (2010). Phosphorylation of Sox2 cooperates in reprogramming to pluripotent stem cells. *Stem Cells* **28**: 2141–2150.
11. Chen, L and Khillan, JS (2010). A novel signaling by vitamin A/retinol promotes self renewal of mouse embryonic stem cells by activating PI3K/Akt signaling pathway via insulin-like growth factor-1 receptor. *Stem Cells* **28**: 57–63.
12. Okita, K, Ichisaka, T and Yamanaka, S (2007). Generation of germline-competent induced pluripotent stem cells. *Nature* **448**: 313–317.
13. Stambolic, V, Suzuki, A, de la Pompa, JL, Brothers, GM, Mirtsos, C, Sasaki, T *et al.* (1998). Negative regulation of PKB/Akt-dependent cell survival by the tumor suppressor PTEN. *Cell* **95**: 29–39.
14. Myers, MP, Pass, I, Batty, IH, Van der Kaay, J, Stolarov, JP, Hemmings, BA *et al.* (1998). The lipid phosphatase activity of PTEN is critical for its tumor supressor function. *Proc Natl Acad Sci USA* **95**: 13513–13518.
15. Sun, H, Lesche, R, Li, DM, Liliental, J, Zhang, H, Gao, J *et al.* (1999). PTEN modulates cell cycle progression and cell survival by regulating phosphatidylinositol 3,4,5,-trisphosphate and Akt/protein kinase B signaling pathway. *Proc Natl Acad Sci USA* **96**: 6199–6204.
16. Salmena, L, Carracedo, A and Pandolfi, PP (2008). Tenets of PTEN tumor suppression. *Cell* **133**: 403–414.
17. Alva, JA, Lee, GE, Escobar, EE and Pyle, AD (2011). Phosphatase and tensin homolog regulates the pluripotent state and lineage fate choice in human embryonic stem cells. *Stem Cells* **29**: 1952–1962.
18. Di Cristofano, A, Pesce, B, Cordon-Cardo, C and Pandolfi, PP (1998). Pten is essential for embryonic development and tumour suppression. *Nat Genet* **19**: 348–355.
19. Higuchi, M, Masuyama, N, Fukui, Y, Suzuki, A and Gotoh, Y (2001). Akt mediates Rac/Cdc42-regulated cell motility in growth factor-stimulated cells and in invasive PTEN knockout cells. *Curr Biol* **11**: 1958–1962.
20. Solter, D and Knowles, BB (1978). Monoclonal antibody defining a stage-specific mouse embryonic antigen (SSEA-1). *Proc Natl Acad Sci USA* **75**: 5565–5569.
21. Maehama, T and Dixon, JE (1998). The tumor suppressor, PTEN/MMAC1, dephosphorylates the lipid second messenger, phosphatidylinositol 3,4,5-trisphosphate. *J Biol Chem* **273**: 13375–13378.
22. Li, DM and Sun, H (1997). TEP1, encoded by a candidate tumor suppressor locus, is a novel protein tyrosine phosphatase regulated by transforming growth factor beta. *Cancer Res* **57**: 2124–2129.
23. Watanabe, S, Umehara, H, Murayama, K, Okabe, M, Kimura, T and Nakano, T (2006). Activation of Akt signaling is sufficient to maintain pluripotency in mouse and primate embryonic stem cells. *Oncogene* **25**: 2697–2707.
24. Kimura, T, Suzuki, A, Fujita, Y, Yomogida, K, Lomeli, H, Asada, N *et al.* (2003). Conditional loss of PTEN leads to testicular teratoma and enhances embryonic germ cell production. *Development* **130**: 1691–1700.
25. Posner, BI, Faure, R, Burgess, JW, Bevan, AP, Lachance, D, Zhang-Sun, G *et al.* (1994). Peroxovanadium compounds. A new class of potent phosphotyrosine phosphatase inhibitors which are insulin mimetics. *J Biol Chem* **269**: 4596–4604.
26. Salh, B, Wagey, R, Marotta, A, Tao, JS and Pelech, S (1998). Activation of phosphatidylinositol 3-kinase, protein kinase B, and p70 S6 kinases in lipopolysaccharide-stimulated Raw 264.7 cells: differential effects of rapamycin, Ly294002, and wortmannin on nitric oxide production. *J Immunol* **161**: 6947–6954.
27. Zhu, S, Li, W, Zhou, H, Wei, W, Ambasudhan, R, Lin, T *et al.* (2010). Reprogramming of human primary somatic cells by OCT4 and chemical compounds. *Cell Stem Cell* **7**: 651–655.
28. Huangfu, D, Maehr, R, Guo, W, Eijkelenboom, A, Snitow, M, Chen, AE *et al.* (2008). Induction of pluripotent stem cells by defined factors is greatly improved by small-molecule compounds. *Nat Biotechnol* **26**: 795–797.
29. Silva, J, Barrandon, O, Nichols, J, Kawaguchi, J, Theunissen, TW and Smith, A (2008). Promotion of reprogramming to ground state pluripotency by signal inhibition. *PLoS Biol* **6**: e253.
30. Lin, T, Ambasudhan, R, Yuan, X, Li, W, Hilcove, S, Abujarour, R *et al.* (2009). A chemical platform for improved induction of human iPSCs. *Nat Methods* **6**: 805–808.
31. Maherali, N, Sridharan, R, Xie, W, Utikal, J, Eminli, S, Arnold, K *et al.* (2007). Directly reprogrammed fibroblasts show global epigenetic remodeling and widespread tissue contribution. *Cell Stem Cell* **1**: 55–70.
32. Zhu, J, Blenis, J and Yuan, J (2008). Activation of PI3K/Akt and MAPK pathways regulates Myc-mediated transcription by phosphorylating and promoting the degradation of Mad1. *Proc Natl Acad Sci USA* **105**: 6584–6589.
33. Hong, H, Takahashi, K, Ichisaka, T, Aoi, T, Kanagawa, O, Nakagawa, M *et al.* (2009). Suppression of induced pluripotent stem cell generation by the p53-p21 pathway. *Nature* **460**: 1132–1135.
34. Liang, G, He, J and Zhang, Y (2012). Kdm2b promotes induced pluripotent stem cell generation by facilitating gene activation early in reprogramming. *Nat Cell Biol* **14**: 457–466.
35. Aparicio, IM, Garcia-Herreros, M, Fair, T and Lonergan, P (2010). Identification and regulation of glycogen synthase kinase-3 during bovine embryo development. *Reproduction* **140**: 83–92.
36. Wang, Q, Xu, X, Li, J, Liu, J, Gu, H, Zhang, R *et al.* (2011). Lithium, an anti-psychotic drug, greatly enhances the generation of induced pluripotent stem cells. *Cell Res* **21**: 1424–1435.
37. Chen, T, Shen, L, Yu, J, Wan, H, Guo, A, Chen, J *et al.* (2011). Rapamycin and other longevity-promoting compounds enhance the generation of mouse induced pluripotent stem cells. *Aging Cell* **10**: 908–911.
38. Kawamura, T, Suzuki, J, Wang, YV, Menendez, S, Morera, LB, Raya, A *et al.* (2009). Linking the p53 tumour suppressor pathway to somatic cell reprogramming. *Nature* **460**: 1140–1144.

39. Utikal, J, Polo, JM, Stadtfeld, M, Maherali, N, Kulalert, W, Walsh, RM *et al.* (2009). Immortalization eliminates a roadblock during cellular reprogramming into iPS cells. *Nature* **460**: 1145–1148.
40. Li, H, Collado, M, Villasante, A, Strati, K, Ortega, S, Cañamero, M *et al.* (2009). The Ink4/Arf locus is a barrier for iPS cell reprogramming. *Nature* **460**: 1136–1139.
41. Banito, A, Rashid, ST, Acosta, JC, Li, S, Pereira, CF, Geti, I *et al.* (2009). Senescence impairs successful reprogramming to pluripotent stem cells. *Genes Dev* **23**: 2134–2139.
42. Marión, RM, Strati, K, Li, H, Murga, M, Blanco, R, Ortega, S *et al.* (2009). A p53-mediated DNA damage response limits reprogramming to ensure iPS cell genomic integrity. *Nature* **460**: 1149–1153.
43. Kim C, Wong J, Wen J, Wang S, Wang C, Spiering S *et al.* (2013). Studying arrhythmogenic right ventricular dysplasia with patient-specific iPSCs. *Nature*. doi:10.1038/nature11799
44. Zhang, J, Nuebel, E, Daley, GQ, Koehler, CM and Teitell, MA (2012). Metabolic Regulation in Pluripotent Stem Cells during Reprogramming and Self-Renewal. *Cell Stem Cell* **11**: 589–595.
45. Britton, JS, Lockwood, WK, Li, L, Cohen, SM and Edgar, BA (2002). Drosophila's insulin/PI3-kinase pathway coordinates cellular metabolism with nutritional conditions. *Dev Cell* **2**: 239–249.
46. Hollander, MC, Blumenthal, GM and Dennis, PA (2011). PTEN loss in the continuum of common cancers, rare syndromes and mouse models. *Nat Rev Cancer* **11**: 289–301.
47. Kitamura, T, Koshino, Y, Shibata, F, Oki, T, Nakajima, H, Nosaka, T *et al.* (2003). Retrovirus-mediated gene transfer and expression cloning: powerful tools in functional genomics. *Exp Hematol* **31**: 1007–1014.
48. Morita, S, Kojima, T and Kitamura, T (2000). Plat-E: an efficient and stable system for transient packaging of retroviruses. *Gene Ther* **7**: 1063–1066.
49. Blelloch, R, Wang, Z, Meissner, A, Pollard, S, Smith, A and Jaenisch, R (2006). Reprogramming efficiency following somatic cell nuclear transfer is influenced by the differentiation and methylation state of the donor nucleus. *Stem Cells* **24**: 2007–2013.
50. Kang, L, Wang, J, Zhang, Y, Kou, Z and Gao, S (2009). iPS cells can support full-term development of tetraploid blastocyst-complemented embryos. *Cell Stem Cell* **5**: 135–138.

PLOS ONE

Establishment of Immortalized Human Erythroid Progenitor Cell Lines Able to Produce Enucleated Red Blood Cells

Ryo Kurita[1], Noriko Suda[1], Kazuhiro Sudo[1], Kenichi Miharada[1], Takashi Hiroyama[1], Hiroyuki Miyoshi[2], Kenzaburo Tani[3], Yukio Nakamura[1]*

1 Cell Engineering Division, RIKEN BioResource Center, Tsukuba, Ibaraki, Japan, **2** Subteam for Manipulation of Cell Fate, RIKEN BioResource Center, Tsukuba, Ibaraki, Japan, **3** Department of Molecular Genetics, Division of Molecular and Clinical Genetics, Medical Institute of Bioregulation, Kyushu University, Higashi-ku, Fukuoka, Japan

Abstract

Transfusion of red blood cells (RBCs) is a standard and indispensable therapy in current clinical practice. In vitro production of RBCs offers a potential means to overcome a shortage of transfusable RBCs in some clinical situations and also to provide a source of cells free from possible infection or contamination by microorganisms. Thus, in vitro production of RBCs may become a standard procedure in the future. We previously reported the successful establishment of immortalized mouse erythroid progenitor cell lines that were able to produce mature RBCs very efficiently. Here, we have developed a reliable protocol for establishing immortalized human erythroid progenitor cell lines that are able to produce enucleated RBCs. These immortalized cell lines produce functional hemoglobin and express erythroid-specific markers, and these markers are upregulated following induction of differentiation in vitro. Most importantly, these immortalized cell lines all produce enucleated RBCs after induction of differentiation in vitro, although the efficiency of producing enucleated RBCs remains to be improved further. To the best of our knowledge, this is the first demonstration of the feasibility of using immortalized human erythroid progenitor cell lines as an ex vivo source for production of enucleated RBCs.

Citation: Kurita R, Suda N, Sudo K, Miharada K, Hiroyama T, et al. (2013) Establishment of Immortalized Human Erythroid Progenitor Cell Lines Able to Produce Enucleated Red Blood Cells. PLoS ONE 8(3): e59890. doi:10.1371/journal.pone.0059890

Editor: Dimas Tadeu Covas, University of Sao Paulo - USP, Brazil

Received November 13, 2012; **Accepted** February 19, 2013; **Published** March 22, 2013

Funding: This work was supported by the project for realization of regenerative medicine in the Ministry of Education, Culture, Sports, Science, and Technology in Japan (MEXT) and other grants from the MEXT. The funders had no role in study design, data collection and analysis, decision to publish, or preparation of the manuscript.

Competing Interests: The authors have declared that no competing interests exist.

* E-mail: yukionak@brc.riken.jp

Introduction

The transfusion of RBCs is a standard clinical therapy. Currently, the supply of RBCs for transfusion is dependent on donation of blood by large numbers of volunteers. This system has two important shortcomings, namely, shortages of volunteers and contamination of donated blood by microorganisms. One promising way around these problems might be to produce RBCs in vitro [1,2,3] from hematopoietic stem/progenitor cells [4,5], embryonic stem (ES) cells [6], or induced pluripotent stem (iPS) cells [7].

Recently, we developed a new approach in the mouse for producing RBCs in vitro [8]. Using mouse ES cells, we successfully established immortalized erythroid progenitor cell lines, which we termed mouse ES cell-derived erythroid progenitor (MEDEP) cell lines, and confirmed that these cell lines could produce mature RBCs in vitro [8]. The logical next step was to create immortalized human erythroid progenitor cell lines that could provide a convenient and reliable ex vivo source for RBC production. These cell lines could also be of value for a range of basic science investigations, for example, into erythroid differentiation and enucleation. The present study shows the feasibility of establishing immortalized human erythroid progenitor cell lines and demonstrates that enucleated RBCs can be induced to differentiate in these cell lines.

Materials and Methods

Cell Lines

Human iPS cell lines (HiPS-RIKEN-3A and HiPS-RIKEN-4A) and the OP9 cell line were obtained from the Cell Engineering Division of RIKEN BioResource Center (Tsukuba, Ibaraki, Japan). iPS cells were maintained in an undifferentiated state in the presence of a feeder cell line, SNL76/7, as described previously [9]. The SNL76/7 feeder cell line was obtained from the European Collection of Cell Cultures (Salisbury, Wiltshire, UK) and cultured in DMEM (Sigma, St. Louis, MO, USA) supplemented with 7.5% fetal bovine serum (FBS; Invitrogen, Carlsbad, CA, USA).

Establishment of Human iPS Cell Lines Expressing TAL1

The internal ribosomal entry site (IRES)-puromycin resistant gene ($Puro^r$) cassette was amplified by polymerase chain reaction (PCR) using pIRESpuro3 plasmid DNA (TAKARA BIO, Otsu, Shiga, Japan) with the following primers: 5′-tga tcc tct aga ctg gaa tta att cgc tgt ctg cga-3′ (sense) and 5′-gtg ggg gtt aac tca ggc acc ggg ctt gcg ggt ca-3′ (anti-sense). After confirmation of the DNA

sequence, the IRES-Puro^r cassette was cloned into the CSII-EF-RfA lentiviral vector plasmid (Figure S1), which contains the human EF-1α promoter and the Gateway system (Invitrogen), to produce CSII-EF-RfA-IRES-Puro^r. TAL1 cDNA and the recombination sequences for the Gateway system (Invitrogen) were amplified by reverse transcription-PCR (RT-PCR) using human fetal liver total RNA purchased from TAKARA BIO with the following primers: 5′-ggg gac aag ttt gta caa aaa agc agg ctt cac cat gac cga gcg gcc gcc gag cga-3′ (sense) and 5′-ggg gac cac ttt gta caa gaa agc tgg gtc tca ccg agg gcc ggc tcc atc ggc-3′ (anti-sense). The RT-PCR amplification product (1060 bp) was subcloned into the pDONR222 vector (Invitrogen) and verified by DNA sequencing. The TAL1 cDNA was then transferred to the CSII-EF-RfA-IRES-Puro^r plasmid using Gateway LR clonase (Invitrogen) to produce CSII-EF-TAL1-IRES-Puro^r. The vesicular stomatitis virus G glycoprotein (VSV-G)-pseudotyped lentiviral vector preparation was performed as described previously [10] with the exception that Fugene HD (Roche, Mannheim, Germany) was used for transfection instead of polyethyleneimine. Human iPS cell lines were transduced with CSII-EF-TAL1-IRES-Puro^r lentiviral vector in the presence of polybrene (8 μg/ml; Sigma) and iPS cells expressing TAL1 were selected using puromycin (2 μg/ml; InvivoGen, San Diego, CA, USA).

Construction of Lentiviral Vector Plasmid for Expression of Human Papilloma Virus Type 16-E6/E7 Using the Tetracycline-inducible System

The CSIV-TRE-RfA-UbC-KT lentiviral vector plasmid (Figure S2) contains the humanized Kusabira-Orange 1 (hKO1) fluorescent protein gene [11] and the reverse tetracycline (Tet)-controlled transcriptional transactivator (TAKARA BIO) linked by the Thosea asigna virus 2A peptide sequence under the control of human ubiquitin C promoter; this plasmid is designed to express cDNA under the control of the Tet-responsive promoter (TAKARA BIO). The human papilloma virus 16 (HPV16)-E6/E7 genomic DNA subcloned into pENTR201 (Invitrogen) was a kind gift of Dr. Kiyono (Division of Virology, Molecular Oncology Group, National Cancer Center Research Institute, Japan). The HPV16-E6/E7 genomic DNA was transferred to the CSIV-TRE-RfA-UbC-KT plasmid using Gateway LR clonase to produce CSIV-TRE-HPV16-E6/E7-UbC-KT. Lentiviral vector preparation was performed as described above.

Specific Factors

The following factors were used in this study: human stem cell factor (SCF; R&D systems, Minneapolis, MN, USA), human erythropoietin (EPO; Kirin Brewery, Tokyo, Japan), human FLT3 ligand (FLT3-L; R&D systems), dexamethasone (DEX; Sigma), human vascular endothelial growth factor (VEGF; R&D systems), human insulin-like growth factor-II (IGF-II; R&D systems), and human thrombopoietin (TPO; R&D systems).

Establishment of Immortalized Erythroid Progenitor Cell Lines from Human iPS Cells Expressing TAL1

The protocol schedule is summarized in Table 1 and a graphical depiction of the process is shown in Figure 1. To induce hematopoietic cells from HiPS-RIKEN-3A-TAL1 and HiPS-RIKEN-4A-TAL1 cells, cells were cultured on OP9 feeder cells in basal differentiation medium composed of IMDM (Sigma) supplemented with 15% fetal bovine serum (FBS; Invitrogen), ITS (10 μg/ml human insulin, 5.5 μg/ml human transferrin, and 5 ng/ml sodium selenite; Sigma), 50 mg/mL ascorbic acid (Sigma), 0.45 mM α-monothioglycerol (Sigma), and PSQ (100 units/ml penicillin, 100 mg/ml streptomycin, and 2 mM L-glutamine; Invitrogen) in the presence of VEGF (20 ng/ml) and IGF-II (200 ng/ml). From day 10, the cells were cultured on OP9 cells in the presence of SCF (50 ng/ml), EPO (3 IU/ml) and DEX (10^{-6} M). On day 16, the HPV16-E6/E7 expression system was introduced into the cells by lentiviral transduction. Four days later, the cells were cultured on OP9 cells in the presence of DOX (1 μg/ml), SCF (50 ng/ml), EPO (3 IU/ml) and DEX (10^{-6} M). The medium was usually changed twice per week, except when cell numbers were low. Around three months after initiation of culture, the cells were able to proliferate without feeder cells. After this time point, we maintained the cells in a serum-free medium, StemSpan SFEM® medium (StemCell Technologies, Vancouver, BC, Canada), in the presence of specific factors.

Establishment of Immortalized Erythroid Progenitor Cell Lines from Human CD34-positive Hematopoietic Stem/progenitor Cells

The protocol schedule is summarized in Table 2 and a graphical depiction of the process is shown in Figure 1. CD34-positive hematopoietic stem/progenitor cells derived from umbilical cord blood were obtained from the Stem Cell Resource Network in Japan (Banks at Miyagi, Tokyo, Kanagawa, Aichi, and Hyogo) through the RIKEN BioResource Center. CD34-positive cells (1×10^5 cells) were cultured in a serum-free medium, StemSpan SFEM® medium (StemCell Technologies), in the presence of SCF (50 ng/ml), TPO (50 ng/ml) and FLT3-L (50 ng/ml). On day 1 of culture, the HPV16-E6/E7 expression system was introduced into the cells by lentiviral transduction. Four days after introduction of the HPV16-E6/E7 expression system, the cells were cultured in the presence of doxycycline (DOX, 1 μg/ml; TAKARA BIO), SCF (50 ng/ml), EPO (3 IU/ml) and DEX (10^{-6} M). DOX was used as a substitute for Tet, and the presence of DOX induced the expression of HPV16-E6/E7. The medium was usually changed twice per week, except when cell numbers were low.

Induction of Differentiation of Immortalized Erythroid Progenitor Cell Lines

The immortalized erythroid progenitor cell lines were induced to differentiate into more mature erythroid cells by culture in erythroid differentiation medium; IMDM (Sigma) containing 10% human AB serum (Kohjin Bio, Saitama, Japan or TAKARA BIO), α-tocopherol (20 ng/ml; Sigma), linoleic acid (4 ng/ml; Sigma), cholesterol (200 ng/ml; Sigma), sodium selenite (2 ng/ml; Sigma), holo-transferrin (200 μg/ml; Sigma), human insulin (10 μg/ml; Sigma), ethanolamine (10 μM; Sigma), 2-ME (0.1 mM; Sigma), D-mannitol (14.57 mg/ml; Sigma), mifepristone (an antagonist of glucocorticoid receptor, 1 μM; Sigma) and EPO (5 IU/ml).

Flow Cytometry

A sample of cells ($<1\times10^6$) was stained with monoclonal antibodies (MoAbs) in 100 μl of staining medium (phosphate buffered saline [PBS; Sigma] containing 2% FBS [Invitrogen] and 0.25% sodium azide [Sigma]) for 30 min on ice. The cells were washed twice with the staining medium, and analyzed using a FACS Calibur (BD Biosciences, San Jose, CA, USA). MoAbs against human antigens were conjugated with fluorescein isothiocyanate (FITC), Alexa Fluor® 488 (Alexa488) or allophycocyanin (APC). FITC-conjugated CD34 (cat. #555821), CD36 (cat. #555454), CD41a (cat. #555466), and CD71 (cat. #555536), Alexa488-conjugated CD11b (cat. #557701) and APC-conjugated

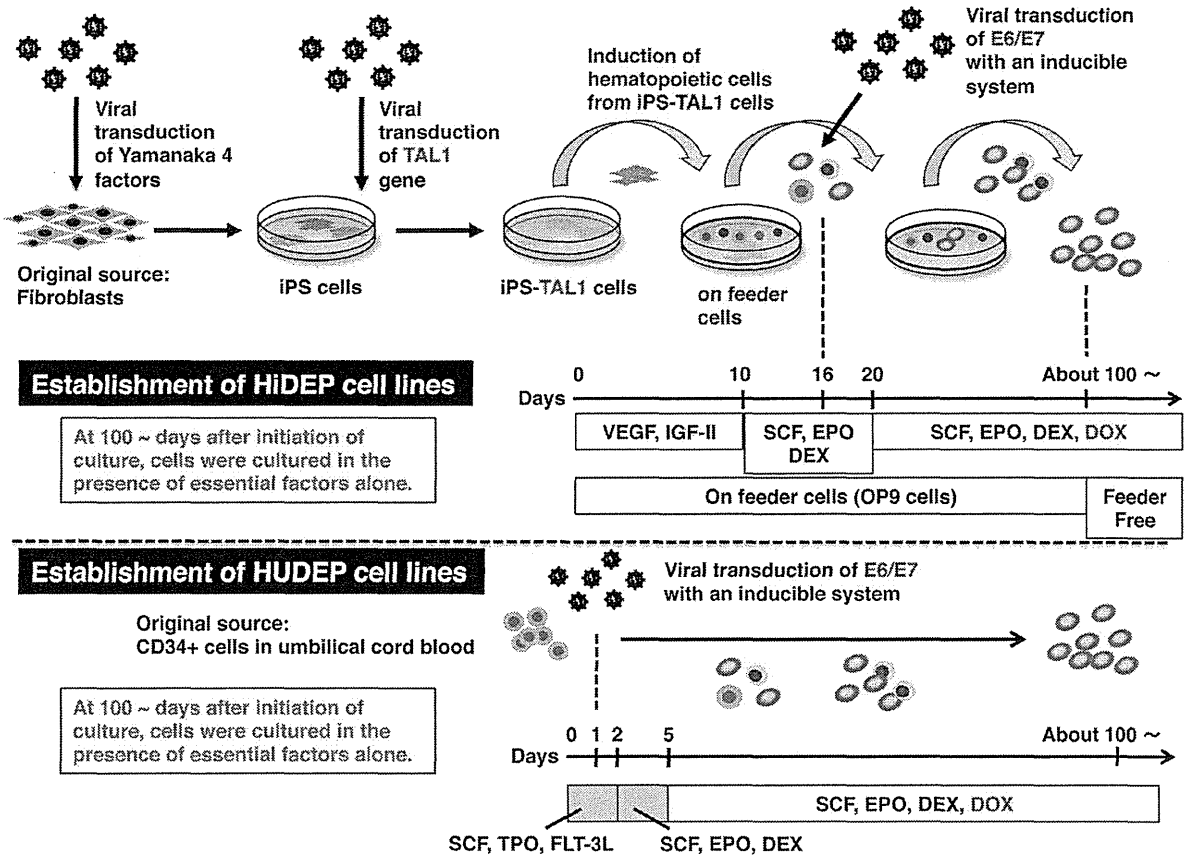

Figure 1. Schematic outline of the procedures for establishing immortalized human erythroid progenitor cell lines from iPS cells and from hematopoietic stem/progenitor cells in umbilical cord blood.
doi:10.1371/journal.pone.0059890.g001

Table 1. An outline of the culture schedule used to establish immortalized cell lines from iPS cells.

Day of culture	Feeder cells	Attached cells	Detached cells	Specific factors used	Doxycycline
Day 0	OP9	(Start)	(Start)	VEGF, IGF-II	(−)
Day 4, 7	OP9[a]	Re-cultured[b]	Discarded	VEGF, IGF-II	(−)
Day 10, 13	OP9[a]	Re-cultured[b]	Re-cultured[c]	SCF, EPO, DEX	(−)
Day 16	OP9[d]	Discarded[d]	Virus infection[e]	SCF, EPO, DEX	(−)
Day 17	OP9[a]	Re-cultured[b]	Re-cultured[c]	SCF, EPO, DEX	(−)
Day 20~[f]	OP9[a or d]	Re-cultured[b] or Discarded	Re-cultured[c, g]	SCF, EPO, DEX	(+)
Day 48, 97~[f]	(−)[h]	Discarded[i]	Re-cultured[g]	SCF, EPO, DEX	(+)
Day 131~[f]	(−)	Discarded[i]	Re-cultured[g]	SCF, EPO, DEX[j]	(+)

Human iPS cells ($4x10^4$) were cultured in the presence of feeder cells with cytokines in a 100 mm dish. Attached cells indicate cells attached to the dish or to the feeder cells. Detached cells indicate cells detached from the dish or from the feeder cells. VEGF, vascular endothelial growth factor. IGF-II, insulin-like growth factor-II. SCF, stem cell factor. EPO, erythropoietin. DEX, dexamethasone.
[a]OP9 feeder cells were used again for a further period.
[b]Attached cells were cultured again on OP9 feeder cells.
[c]All detached cells collected from the dish were cultured again in fresh medium.
[d]Used OP9 cells were discarded together with any attached cells and a fresh batch of OP9 cells were used for the next culture step.
[e]All detached cells collected from the dish were infected with lentivirus expressing HPV16-E6/E7, and were then cultured again.
[f]The medium was changed twice per week.
[g]Detached cells from the dish were either all re-cultured or some re-cultured and the remainder stored for further analyses.
[h]From this time point, the detached cells could proliferate without feeder cells.
[i]Very few attached cells were detected.
[j]At approximately day 131, the requirement for essential factors for proliferation was evaluated.
doi:10.1371/journal.pone.0059890.t001

Table 2. An outline of the culture schedule used to establish immortalized cell lines from hematopoietic stem/progenitor cells.

Day of culture	Attached cells	Detached cells	Specific factors used	Doxycycline
Day 0	(Start)	(Start)	SCF, TPO, FLT3-L	(−)
Day 1	Not detected	Virus infection[a]	SCF, TPO, FLT3-L	(−)
Day 2	Not detected	Re-cultured[b]	SCF, EPO, DEX	(−)
Day 5, 8	Discarded[c]	Re-cultured[b]	SCF, EPO, DEX	(+)
Day 11~[d]	Discarded[c]	Re-cultured[e]	SCF, EPO, DEX	(+)
Day 110~[d]	Discarded[c]	Re-cultured	SCF, EPO, DEX[f]	(+)

$CD34^+$ cells (1×10^5) were cultured in the absence of feeder cells with cytokines in the well of a 24-well plate or in a 100 mm dish. SCF, stem cell factor. EPO, erythropoietin. FLT3-L, FLT3 ligand. DEX, dexamethasone.
[a]All cells collected from the dish were infected with lentivirus expressing HPV16-E6/E7 and then cultured again.
[b]All cells collected from the dish were cultured again.
[c]Very few attached cells were detected.
[d]The medium was changed twice per week.
[e]Detached cells collected from the dish were either all cultured again or only some were re-cultured and the remainder were stored for further analysis.
[f]At approximately Day 110, the cultures were evaluated for the essential factor(s) for proliferation.
doi:10.1371/journal.pone.0059890.t002

CD33 (cat. #551378), CD45 (cat. #555485), c-KIT (cat. #550412), glycophorin A (GPA) (cat. #551336) and HLA-ABC (cat. #555555) were purchased from BD Biosciences. FITC-conjugated mouse IgG_1 (cat. #555748), IgM (cat. #555583), APC-conjugated mouse IgG_1 (cat. #555751) and IgG_{2b} (cat. #555745) were also purchased from BD Biosciences and used as isotype controls. Cell viability was monitored by propidium iodide (PI; Sigma) staining. Flow cytometry data was analyzed using CellQuest analysis software (BD Biosciences). In this analysis, PI-positive cells were excluded as being dead and PI-negative cells were analyzed as being viable.

Functional Analysis of Hemoglobin

Following induction of differentiation of immortalized erythroid progenitor cells (5×10^7 cells) for 4 to 6 days, the cells were collected, washed with PBS, and subjected to analysis. Oxygen equilibrium curves were determined using a Hemox-Analyzer Model B (TSC Scientific, New Hope, PA). The gas phase gradients were obtained using nitrogen and room air, and the curves were run in both directions. Human peripheral blood cells and umbilical cord blood cells were used as the controls.

Quantitative Reverse Transcription-polymerase Chain Reaction (qRT-PCR)

Total RNA was extracted from cells using ISOGEN™ reagent (Wako, Osaka, Japan). Reverse transcription was carried out using 4.5 μg total RNA and the SuperScript®III First Strand Synthesis System (Invitrogen) in a 20 μl reaction volume. After reverse transcription, 180 μl of water was added to the reaction mixture and a 1 μl aliquot was used for each PCR. PCR was carried out using FastStart TaqMan® Probe Master and Universal ProbeLibrary Probes (Roche, Mannheim, Germany). PCR products were monitored by FAM (CarboxyFluorescein) dye fluorescence using a Thermal Cycler Dice® Real Time System (Takara Bio). Glyceraldehyde-3-phosphate dehydrogenase (GAPDH) amplification was used as the internal control.

Primers and Probes

The following primers and probes were used in this study: human GATA1, sense primer 5′-cac tga gct tgc cac atc c-3′ and antisense primer 5′-atg gag cct ctg ggg att a-3′ (Probe #26); human GATA2, sense primer 5′-aag gct cgt tcc tgt tca ga-3′ and antisense primer 5′-ggc att gca cag gta gtg g-3′ (Probe #70); human GFI1B, sense primer 5′-cct ctt gtg ccc agc act-3′ and antisense primer 5′-cgt gag ggg tgg aga aga c-3′ (Probe #41); human EKLF, sense primer 5′-aca cca aga gct ccc acc t-3′ and antisense primer 5′-gta gtg gcg ggt cag ctc-3′ (Probe #7); human EPO receptor (EPOR), sense primer 5′-ttg gag gac ttg gtg tgt ttc-3′ and antisense primer 5′-agc ttc cat ggc tca tcc t-3′ (Probe #69); human α-globin, sense primer 5′-gac ccg gtc aac ttc aag c-3′ and antisense primer 5′-aga agc cag gaa ctt gtc ca-3′ (Probe #10); human β-globin, sense primer 5′-gca cgt gga tcc tga gaa ct-3′ and antisense primer 5′-cac tgg tgg ggt gaa ttc tt-3′ (Probe #61); human γ-globin, sense primer 5′-tgg atc ctg aga act tca agc-3′ and antisense primer 5′-gcc act gca gtc acc atc t-3′ (Probe #72); human c-MYB, sense primer 5′-agc aag gtg cat gat cgt c-3′ and antisense primer 5′-gat cac acc atg atg aag aat cag-3′ (Probe #37); human SOX6, sense primer 5′-gct tct gga ctc agc cct tt-3′ and antisense primer 5′-gga gtt gat ggc atc ttt gc-3′ (Probe #67); human BCL11A, sense primer 5′-ccc aaa cag gaa cac ata gca-3′ and antisense primer 5′-gag ctc cat gtg cag aac g-3′ (Probe #52); human TAL1 (to detect endogenous TAL1 gene), sense primer 5′-tgt gtg aga gac ggt gtc ttg-3′ and antisense primer 5′-caa ggc tgc aga cag caa-3′ (Probe #19); human Band 3, sense primer 5′-tct tca gga acg tgg agc tt-3′ and antisense primer 5′-cct cat caa agg ttg cct tg-3′ (Probe #89); human Band 4.1, sense primer 5′-cca cac tga gac caa gac ca-3′ and antisense primer 5′-cca agt ctc cac tgt tgt cgt-3′ (Probe #44); human Ankyrin-1, sense primer 5′-gag cac gag gag gtg act gt-3′ and antisense primer 5′-gtg tcg agg tgt gat cct tg-3′ (Probe #65); human α-Spectrin, sense primer 5′-gct ttg aaa ggg acc tcg ta-3′ and antisense primer 5′-ctc tgc tgt ctc ccc cag t-3′ (Probe #14); human GAPDH, sense primer 5′-agc cac atc gct cag aca c-3′ and antisense primer 5′-gcc caa tac gac caa atc c-3′ (Probe #60).

Morphological Analysis and Cell Staining

Cell morphologies were assessed using smears prepared on microscope slides or attached to microscope slides using a Cytospin 3 (Thermo Electron Corporation, Waltham, MA, USA). The cells were stained with Diff-Quik (Sysmex International, Kobe, Japan) and analyzed by microscopy.

Cell size and cell viability were measured using an automated cell counter, ViCell™ (Beckman Coulter, Fullerton, CA, USA).

Supravital staining was performed by incubating the cells in 0.3% new methylene blue solution (Muto Pure Chemicals, Tokyo, Japan) at room temperature for 20 min.

Immunostaining with GPA antibody was performed as reported previously [12]. Cells were spun onto microscope slides, washed with PBS(−) (PBS free of Ca and Mg) and fixed in 2% paraformaldehyde/PBS on ice for 10 min. After fixation, the cells were washed three times with PBS(−). Nonspecific binding was blocked with 2% BSA/PBS for 1–3 hr. Samples were incubated at 4°C overnight with mouse monoclonal biotinylated anti-human GPA antibody (R&D systems) diluted to 1:200 in blocking solution. At the same time, SYTO16 solution (Invitrogen), which is a cell membrane-permeable fluorochrome dye that stains nucleic acids, was added to the staining mixture at a final concentration of 0.5 μM. After extensive washing with PBS(−), the cells were incubated with Alexa 647-conjugated streptavidin for 30 min to 1 hr to detect the biotinylated anti-human GPA antibody bound to the cells. After washing, the cells were observed with an LSM780 laser scanning microscope (Carl Zeiss, Oberkochen, Germany).

Benzidine staining was performed using the Peroxidase Stain DAB Kit (Nacalai Tesque, Kyoto, Japan) according to the manufacturer's instructions. After staining, coverslips were mounted using Vectashield containing DAPI (Vector Laboratories, Burlingame, CA, USA) in order to identify nucleated and enucleated cells.

Results

Establishment of Immortalized Erythroid Progenitor Cell Lines from Human iPS Cells

Initially, we attempted to establish immortalized human erythroid progenitor cell lines from human ES cells and iPS cells using essentially the same protocol as for the successful establishment of MEDEP cell lines from mouse ES cells [8]. Three human ES cell lines and two human iPS cell lines were used in these experiments but none yielded abundant erythroid cells although some hematopoietic cells were induced. Thus, the protocol for establishing MEDEP cell lines failed to establish immortalized erythroid progenitor cell lines from human pluripotent stem cell lines.

Next, we investigated whether enforced expression of the transcription factor TAL1 might enable establishment of immortalized erythroid progenitor cell lines. TAL1 plays essential roles in early hematopoiesis [13] and differentiation of erythroid cells and megakaryocytes [14,15]. In an earlier study, we also showed that its expression improved the efficiency of inducing hematopoietic cells from common marmoset ES cells [12]. Therefore, we forced expression of TAL1 in human iPS cell lines (HiPS) [16] and established sub-lines, HiPS-TAL1. HiPS-TAL1 cells showed a significant improvement in the efficiency of induction of hematopoietic cells when grown on OP9 feeder cells in the presence of insulin-like growth factor-II (IGF-II) and vascular endothelial growth factor (VEGF) (Figure 2). Long-term cultures of HiPS-TAL1 cells were also initiated on OP9 cells in the presence of stem cell factor (SCF), erythropoietin (EPO) and thrombopoietin (TPO). The cells proliferated continuously and no longer required OP9 cells after they had been in culture for approximately three months. As a result, we were able to establish six immortalized cell lines that proliferated continuously for more than 1 year. However, these cell lines expressed few hematopoietic cell markers and did not differentiate into more mature cells (data not shown).

Immortalized erythroid progenitor cell lines can be established by transformation of erythroid progenitor cells with the HPV16-derived proteins HPV16-E6/E7 [17]. These cell lines do not produce mature erythrocytes, such as enucleated RBCs, possibly because continuous expression of HPV16-E6/E7 inhibits terminal differentiation of the cells.

In order to test this possibility, we used a Tet-inducible expression system [18,19] to control expression of HPV16-E6/E7 in iPS-derived hematopoietic progenitor cells and investigated whether such expression inhibited establishment of immortalized erythroid progenitor cell lines. Hematopoietic cells were induced from HiPS-TAL1 cells that had been in culture for 16 days (see Materials and methods); the cells were infected with the lentiviral vector containing the Tet-inducible expression system for HPV16-E6/E7. One day after viral infection, the cells were transferred to a new culture on OP9 cells in the presence of SCF, EPO and dexamethasone (DEX) for 3 days. The cells were then cultured in the presence of SCF, EPO, DEX and doxycycline (DOX) over a prolonged period with regular changes of medium. DOX was used as a substitute for Tet, and the presence of DOX induced expression of HPV16-E6/E7. The cells proliferated continuously for more than 1 year; thus, we succeeded in establishing immortalized cell lines. Two cell lines were established from two independent trials using two different HiPS-TAL1 cell lines. We designated these cells as human iPS cell-derived erythroid progenitor (HiDEP) cell lines. HiDEP-1 and HiDEP-2 were established from HiPS-RIKEN-4A and HiPS-RIKEN-3A, respectively.

Establishment of Immortalized Erythroid Progenitor Cell Lines from CD34-positive Hematopoietic Cells in Human Umbilical Cord Blood

As it would be more convenient if immortalized human erythroid progenitor cell lines could be established without recourse to ES or iPS cells, we investigated whether our protocol could be applied to the CD34-positive hematopoietic stem/progenitor cells in umbilical cord blood. CD34-positive cells were collected from umbilical cord blood and cultured in the presence of SCF, TPO and FLT3-ligand (FLT3-L) for 1 day; the cells were then infected with the lentiviral vector containing the Tet-inducible expression system for HPV16-E6/E7. One day after viral infection, the cells were cultured with SCF, EPO and DEX for 4 days. Non-adherent cells were then collected and cultured in the presence of SCF, EPO, DEX and DOX over a prolonged period with regular changes of medium. The cells proliferated continuously for more than 1 year; thus, we also succeeded in establishing immortalized hematopoietic cell lines from umbilical cord blood cells as well. In total, three cell lines were established from three independent trials using three different cord blood samples. We designated these cells as human umbilical cord blood-derived erythroid progenitor (HUDEP) cell lines, HUDEP-1, HUDEP-2 and HUDEP-3.

Dependency on Externally Supplied Culture Factors

The HiDEP and HUDEP cell lines varied in their dependency on externally supplied culture factors (Table S1); thus, for example, the survival and proliferation of HiDEP-1 cells were dependent on DOX (HPV16-E6/E7) and EPO, and partially dependent on DEX but not on SCF (Figure 3A) and the HUDEP-1 cells were dependent on DOX and SCF and partially dependent on EPO but not on DEX (Figure 3B). After confirmation of these dependencies, all cell lines were cultured in the presence of essential factors alone for each cell line.

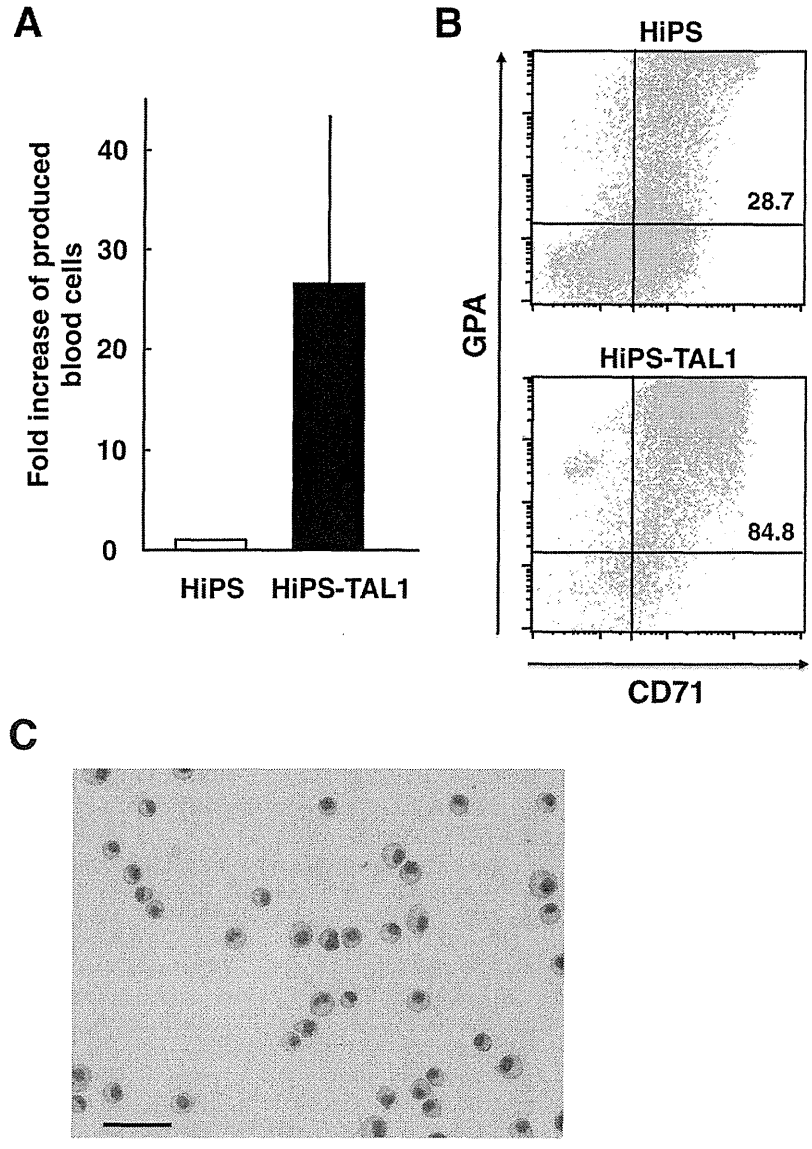

Figure 2. Effect of enforced expression of a transcription factor, TAL1, on induction of hematopoietic cells from human iPS cells. HiPS, human iPS cells (HiPS-RIKEN-3A). HiPS-TAL1, HiPS cells expressing TAL1 (HiPS-RIKEN-3A-TAL1). The cells were analyzed after the induction of differentiation of hematopoietic cells for 15 days. (A) Fold increase of production of hematopoietic cells from HiPS-TAL1 cells compared to HiPS cells. (B) Flow cytometer analysis. CD71, transferrin receptor. Glycophorin A (GPA), an erythroid specific marker. Percentages of GPA-positive cells are indicated in the figure. (C) Morphology of the cells derived from HiPS-TAL1 cells. Scale bar indicates 50 μm. The comparison of HiPS-RIKEN-4A and HiPS-RIKEN-4A-TAL1 showed similar results.
doi:10.1371/journal.pone.0059890.g002

To date, all of the cell lines have continued to proliferate vigorously with no indication of slowdown in cell division rates. We also confirmed that cultures could be re-established after freeze-thaw cycles for all cell lines. Below, we describe the characteristics of the cell lines after continuous culture for more than 6 months and after more than 80 cell division cycles.

Expression of Cell Surface Molecules

Flow cytometric analyses demonstrated that both HiDEP-1 and HiDEP-2 cells expressed the erythroid-specific cell surface marker glycophorin A (GPA) at a high level (Figure 4A), while other hematopoietic cell markers, such as CD11b, CD33, CD34, CD41a and CD45, were not detectable (Figure S3A). CD36 and c-KIT (CD117), markers of immature erythroid cells, were detected at very low levels (Figure 4A and Figure S3A).

All three HUDEP cell lines expressed CD71, glycophorin A, CD36 and c-KIT (Figure 4B). In contrast to the HiDEP cell lines, HUDEP cell lines expressed CD33 and CD45 at various levels, although non-erythroid markers such as CD11b and CD41a were not detectable (Figure S3B). This difference between HiDEP and HUDEP cells might be due to the fact that HiDEP cell lines were established from cells expressing TAL1. To determine whether this was the case, we forced

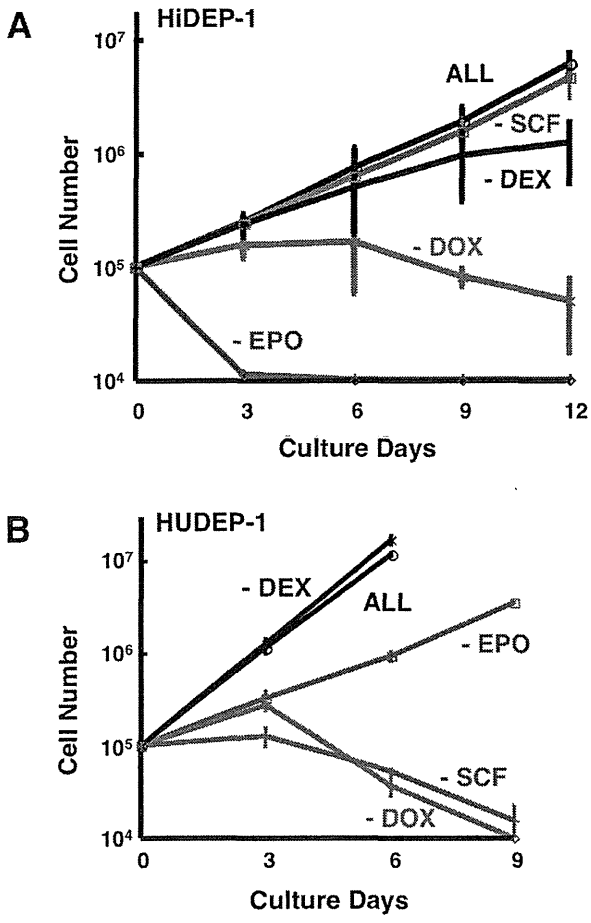

Figure 3. Dependency of the established erythroid progenitor cell lines on externally supplied culture factors. (A) The survival and proliferation of HiDEP-1 cells are dependent on DOX (HPV16-E6/E7) and EPO and partially dependent on DEX. (B) The survival and proliferation of HUDEP-1 cells are dependent on DOX (HPV16-E6/E7) and SCF and partially dependent on EPO. (A, B) DOX, doxycycline; expression of HPV16-E6/E7 is induced by DOX. SCF, stem cell factor. EPO, erythropoietin. DEX, dexamethasone. ALL, cells were cultured in the presence of DOX, SCF, EPO and DEX. –DOX, –SCF, –EPO, –DEX, cells were cultured after deprivation of DOX, SCF, EPO and DEX, respectively. Dependencies of other cell lines on externally supplied culture factors are summarized in Table S1.
doi:10.1371/journal.pone.0059890.g003

expression of TAL1 in HUDEP-1 cells at 7 days after induction of HPV16-E6/E7 expression and established the cell line HUDEP-1-TAL1. However, the phenotype and characteristics of HUDEP-1-TAL1 cells were quite similar to those of HUDEP-1 cells (Figure 4B and Figure S3B).

Induction of Differentiation

Next, we examined whether HiDEP and HUDEP cells could differentiate into more mature stages and produce enucleated RBCs. We found that differentiation could be induced by culturing the HiDEP and HUDEP cells in an erythroid differentiation medium in the presence of EPO alone (see Materials and methods).

Production of Hemoglobin

Upon centrifugation, the HiDEP-1 cells produced a red cell pellet even before the induction of differentiation (Figure 5A) suggesting a continuous and abundant production of hemoglobin. In contrast, upon centrifugation, the HUDEP-1 cells yielded a light orange cell pellet before the induction of differentiation and a red cell pellet after the induction of differentiation (Figure 5B) suggesting that hemoglobin synthesis was upregulated following differentiation.

Functional Analysis of Hemoglobin Produced in HiDEP and HUDEP Cells

We used a Hemox-Analyzer to measure the oxygen binding and dissociation abilities of the hemoglobin produced in mature cells derived from the HiDEP and HUDEP cells [20,21]. Although the oxygen binding and dissociation curves obtained with HiDEP- and HUDEP-derived cells differed between cell lines, they showed similar curves to those obtained with adult peripheral blood or umbilical cord blood (Figure 6). The variation among the curves may be due to the types of hemoglobin expressed in each cell line, i.e., adult type hemoglobin, fetal type hemoglobin or mixture of both types (see below). Apart from this variation, the data indicate that HiDEP and HUDEP cells can produce hemoglobin with oxygen binding and dissociation abilities equivalent to red blood cells produced in vivo.

Analysis of Gene Expression

Gene expression profiles were analyzed by quantitative RT-PCR (qRT-PCR) before and after the induction of differentiation in the HiDEP and HUDEP cells lines. The erythroid-specific markers GATA1, EKLF, GFI1B, TAL1 and EPOR were detected in all cell lines and their expression profiles before and after differentiation were similar to those of cultured erythroid cells derived from umbilical cord blood (Figure 7). This was also the case for c-MYB and SOX6, which are markers of definitive erythroid cells [22,23,24]. In addition, we detected upregulation of the erythroid membrane genes, Band 3, Band 4.1, Ankyrin-1 and α-Spectrin in all cell lines after differentiation (Figure 7).

After differentiation, we found upregulation of α-globin in all cell lines, upregulation of β-globin only in the HUDEP-2 cell line, and upregulation of γ-globin in all cell lines except HUDEP-2. Of note, BCL11A, a repressor of γ-globin expression [25] and critical mediator of globin switching [26], was abundantly detected only in the HUDEP-2 cell line in which β-globin was up-regulated after differentiation (Figure 7).

Cell Viability and Cell Size

After the induction of differentiation in HiDEP-1 cells, the proportion of viable cells decreased but more than half of the cells were still viable 14 days after differentiation (Figure 8A). The average cell size after differentiation decreased compared to undifferentiated cells and the proportion of cells with a diameter less than 10 μm increased from about 20% to approximately 40% (Figure 8A) indicating the increase of very mature erythroid cells.

After the induction of differentiation in HUDEP-1 cells, the frequency of viable cells was considerably reduced compared to HiDEP-1 cells (Figure 8B). However, among viable cells average cell sizes decreased rapidly for two days after differentiation compared to undifferentiated cells, and the proportion of cells with a diameter less than 10 μm increased from about 10% to about 50% (Figure 8B) indicating the increase of very mature erythroid cells. To improve viability, the cells were cultured on OP9 feeder cells and a morphological analysis was performed.

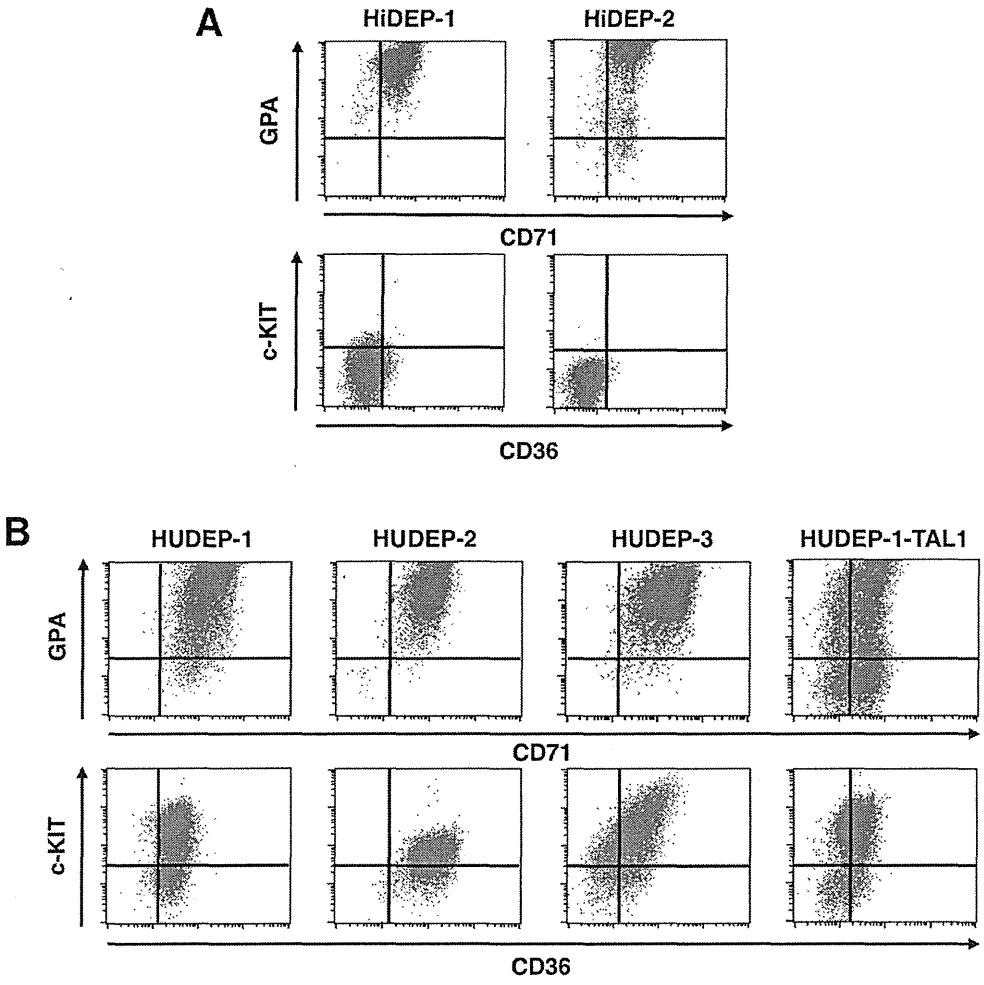

Figure 4. Flow cytometer analyses of the established erythroid progenitor cell lines. (A) Representative results of HiDEP cells. (B) Representative results of HUDEP cells and HUDEP-1 expressing TAL1, HUDEP-1-TAL1. (A, B) GPA, glycophorin A. CD71, transferrin receptor. c-KIT, the receptor of SCF. CD36, a marker of immature erythroid cells.
doi:10.1371/journal.pone.0059890.g004

Morphological Changes during Differentiation

Before the induction of differentiation, both HiDEP-1 and HUDEP-1 cells had round, erythroblast-like morphologies (Figure 9A, B). After the induction of differentiation in HiDEP-1 cells, enucleating cells (arrowheads in Figure 9A) and enucleated cells (black arrows in Figure 9A) were observed from about 7 days after differentiation. Since the cultures contained various types of cell and cell components such as enucleated cells, extruded nuclei after the enucleation process, nucleated cells, dead cells, and cell debris, it was very difficult to accurately calculate the frequency of enucleated cells even by flow cytometrical and morphological analyses. However, at approximately 12 days after the induction of differentiation a considerable number of enucleated cells were present (Figure 9A). The second cell line, HiDEP-2, could also differentiate into more mature cells and produce enucleated RBCs after the induction of differentiation; however, the efficiency of differentiation was lower compared to HiDEP-1 (data not shown).

After the induction of differentiation in HUDEP-1 cells, the morphology of the cells clearly changed and mature and enucleating cells (arrowheads in Figure 9B) and enucleated cells (black arrows in Figure 9B) were observed from about day 6 of differentiation. Although the numbers of enucleated cells were much lower than those induced from HiDEP-1 cells, we did observe reproducible production of enucleated cells. The other HUDEP cell lines, HUDEP-2 and HUDEP-3, could also differentiate into more mature cells and produce enucleated RBCs after the induction of differentiation; the efficiencies of differentiation were almost identical to HUDEP-1 (data not shown).

Confirmation of Enucleated Cells

In general, in vitro produced enucleated RBCs are spherical reticulocytes and not fully mature biconcave cells. To confirm that these enucleated cells were reticulocytes, we performed supravital staining, immunostaining and benzidine staining. The supravital staining demonstrated the presence of reticulocytes (arrows in Figure 10A). In addition, we observed GPA-positive enucleated

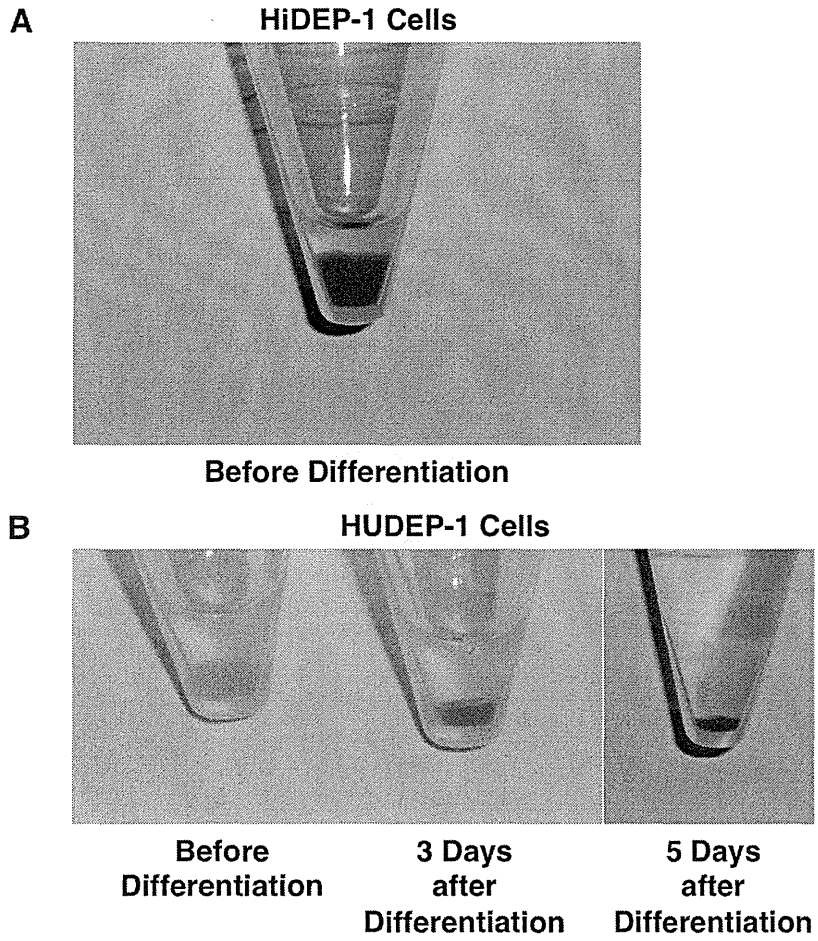

Figure 5. Cell pellets of the established erythroid progenitor cell lines. (A) HiDEP-1 cells before the induction of differentiation. (B) HUDEP-1 cells before and after the induction of differentiation. HUDEP-1 cells were cultured in erythroid differentiation medium on OP9 feeder cells to maintain cell viability during the differentiation process. All other cell lines also showed red cell pellets after the induction of differentiation.
doi:10.1371/journal.pone.0059890.g005

cells (pink cells in Figure 10B) and benzidine-positive enucleated cells (brown cells in Figure 10C).

Discussion

We previously succeeded in establishing MEDEP cell lines from mouse ES cells and were able to induce enucleated RBC production in these cell lines. However, the protocol developed for mouse cell lines failed to establish immortalized erythroid progenitor cell lines from human ES cells and human iPS cells. This difficulty may be related to the fact that in general it is more difficult to establish immortalized human cell lines than immortalized mouse cell lines. The failure of the original protocol led us to alter our strategy for establishing human erythroid progenitor cell lines.

The principal change to our strategy was to use inducible expression of HPV16-E6/E7 in transfected hematopoietic stem/progenitor cells. Through this approach, we developed a method that enabled establishment of immortalized human erythroid progenitor cell lines that possess the ability to differentiate. In iPS cells, the enforced expression of TAL1 supported the process of obtaining cell lines with hematopoietic potential by increasing the number of induced erythroid cells. To date, we have successfully established immortalized cell lines in all trials with this method. All of the immortalized cell lines we described in this study could differentiate into more mature RBCs including enucleated RBCs. The hemoglobin produced in these cell lines possessed similar oxygen binding properties to the hemoglobin in normal RBCs produced in vivo. To our knowledge, this is the first report describing the establishment of immortalized human erythroid progenitor cell lines able to produce enucleated RBCs ex vivo. Although erythroid progenitor cell lines have previously been established using HPV16-E6/E7, these cell lines did not produce enucleated RBCs [17]. One possible explanation for this failure is the continuous expression of HPV16-E6/E7 in these cells. Since efficient differentiation of cells generally requires cell cycle arrest, the continuous expression of HPV16-E6/E7 might have inhibited terminal differentiation of the cells.

The cell lines obtained in this study displayed different efficiencies for producing enucleated RBCs in vitro as is illustrated by comparison of HiDEP and HUDEP cells. We previously found that the efficiency of enucleated RBC production by MEDEP cells improved in vivo after transplantation [8]. Therefore, it is highly